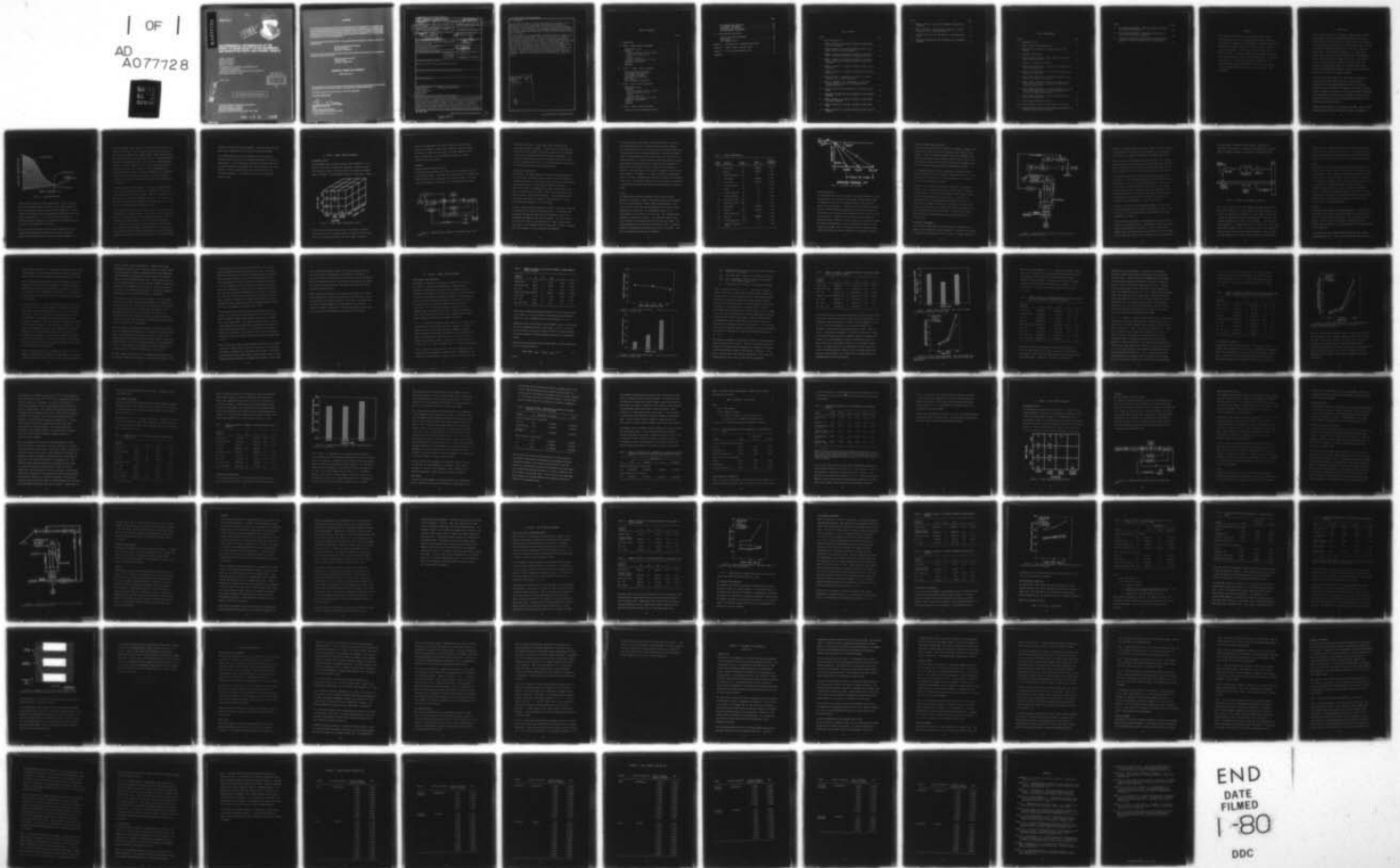


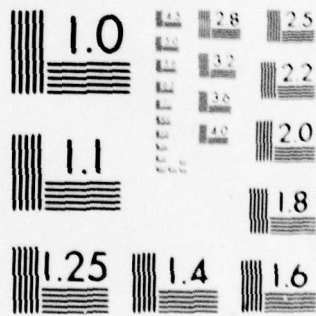
AD-A077 728

VIRGINIA POLYTECHNIC INST AND STATE UNIV BLACKSBURG --ETC F/G 5/8
AN EXPERIMENTAL DETERMINATION OF THE EFFECT OF IMAGE QUALITY ON--ETC(U)
AUG 79 J C GUTMANN , H L SNYDER , W W FARLEY F33615-76-C-5022
AMRL -TR-79-51 NL

UNCLASSIFIED

| OF |
AD
A077728





MICROCOPY RESOLUTION TEST CHART
NATIONAL BUREAU OF STANDARDS-1963-A

AD A 077728

AMRL-TR-79-51

LEVEL *FF*



AN EXPERIMENTAL DETERMINATION OF THE EFFECT OF IMAGE QUALITY ON EYE MOVEMENTS AND SEARCH FOR STATIC AND DYNAMIC TARGETS

JAMES C. GUTMANN
HARRY L. SNYDER
WILLARD W. FARLEY
JOHN E. EVANS, III

DEPARTMENT OF INDUSTRIAL ENGINEERING AND
OPERATIONS RESEARCH
VIRGINIA POLYTECHNIC INSTITUTE & STATE UNIVERSITY
BLACKSBURG, VIRGINIA, 24061

AUGUST 1979

DDC
RECEIVED
DEC 7 1979
A

DDC FILE COPY

Approved for public release; distribution unlimited.

AEROSPACE MEDICAL RESEARCH LABORATORY
AEROSPACE MEDICAL DIVISION
AIR FORCE SYSTEMS COMMAND
WRIGHT-PATTERSON AIR FORCE BASE, OHIO 45433

79 12 6 100

NOTICES

When US Government drawings, specifications, or other data are used for any purpose other than a definitely related Government procurement operation, the Government thereby incurs no responsibility nor any obligation whatsoever, and the fact that the Government may have formulated, furnished, or in any way supplied the said drawings, specifications, or other data, is not to be regarded by implication or otherwise, as in any manner licensing the holder or any other person or corporation, or conveying any rights or permission to manufacture, use, or sell any patented invention that may in any way be related thereto.

Please do not request copies of this report from Aerospace Medical Research Laboratory. Additional copies may be purchased from:

National Technical Information Service
5285 Port Royal Road
Springfield, Virginia 22161

Federal Government agencies and their contractors registered with Defense Documentation Center should direct requests for copies of this report to:

Defense Documentation Center
Cameron Station
Alexandria, Virginia 22314

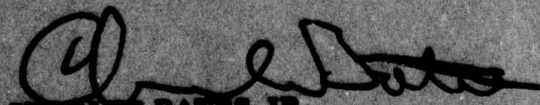
TECHNICAL REVIEW AND APPROVAL

AMRL-TR-79-51

This report has been reviewed by the Information Office (OI) and is releasable to the National Technical Information Service (NTIS). At NTIS, it will be available to the general public, including foreign nations.

This technical report has been reviewed and is approved for publication.

FOR THE COMMANDER



CHARLES BATES, JR.
Chief
Human Engineering Division
Aerospace Medical Research Laboratory

SECURITY CLASSIFICATION OF THIS PAGE (When Data Entered)

18 19 REPORT DOCUMENTATION PAGE		READ INSTRUCTIONS BEFORE COMPLETING FORM	
1. REPORT NUMBER AMRL TR-79-51	2. GOVT ACCESSION NO. 9 Mechanical Dept. 11 Sep 75-	3. RECIPIENT'S CATALOG NUMBER 11 Jan 73	
4. TITLE (and Subtitle) AN EXPERIMENTAL DETERMINATION OF THE EFFECT OF IMAGE QUALITY ON EYE MOVEMENTS AND SEARCH FOR STATIC AND DYNAMIC TARGETS.		5. TYPE OF REPORT & PERIOD COVERED TR 09/11/75-06/11/77	
		6. PERFORMING ORG. REPORT NUMBER	
7. AUTHOR 10 James C. Gutmann Harry L. Snyder Willard W. Farley John E. Evans, III		8. CONTRACT OR GRANT NUMBER(s) 15 F33615-76-C-5022	
9. PERFORMING ORGANIZATION NAME AND ADDRESS Dept. of Industrial Engineering & Opers. Research Virginia Polytechnic Institute & State University Blacksburg, VA 24061		10. PROGRAM ELEMENT / PROJECT, TASK AREA & WORK UNIT NUMBERS 17 62202F 7184-11-05	
11. CONTROLLING OFFICE NAME AND ADDRESS Human Engineering Division Aerospace Medical Research Laboratory (AMRL/HEA) Wright-Patterson AFB, OH 45433		12. REPORT DATE 11 August 1979	
		13. NUMBER OF PAGES 94	
14. MONITORING AGENCY NAME & ADDRESS (if different from Controlling Office) 12 94		15. SECURITY CLASS. (of this report) unclassified	
		15a. DECLASSIFICATION/DOWNGRADING SCHEDULE	
16. DISTRIBUTION STATEMENT (of this Report) Approved for public release; distribution unlimited			
17. DISTRIBUTION STATEMENT (of the abstract entered in Block 20, if different from Report)			
18. SUPPLEMENTARY NOTES			
19. KEY WORDS (Continue on reverse side if necessary and identify by block number) Human Engineering Modulation Transfer Function Image Quality Target Acquisition Eye Movements Television			
20. ABSTRACT (Continue on reverse side if necessary and identify by block number) This report contains the results of two experiments which investigated the effects of the quality of a televised image on eye movements and search-related dependent measures. The first experiment search task involved having subjects perform an air-to-ground search during a simulated flight. The quality of the image presented was varied by either passing, low-pass filtering, or attenuating the video signal and by adding electrical white noise to the video signal. The results of this experiment indicate that (1) at the highest level of electrical noise added, the percent of correct target acquisitions was decreased moderately,			

DD FORM 1 JAN 73 1473

SECURITY CLASSIFICATION OF THIS PAGE (When Data Entered)

406747

Handwritten mark resembling a stylized 'X' or signature.

20. (Continued)

(2) the larger the target, the higher the percent correct responses, (3) the low-pass filtering of the video signal led to shorter ground ranges at acquisition for the large-sized targets, and (4) that the larger the target, the longer the fixation duration. Low to moderate correlations between modulation transfer function area (MTFA) and performance measures generally indicated that as MTFA increases performance improves, and that as MTFA increases fixation duration decreases.

The search task of the second experiment consisted of having the subjects search for a designated letter or numeral across a televised picture of randomly positioned letters and numerals. The quality of the picture was varied by either passing, low-pass filtering, high-pass filtering, or attenuating the video signal and by adding electrical white noise to the video signal. The results of this experiment indicated that (1) the high-pass filtered high noise level condition led to significantly longer search times; and (2) the fixation times associated with the high-pass filtered condition were longer than those associated with the low-pass filtered, attenuated, and unfiltered unattenuated conditions, and that this effect was most pronounced under high noise level conditions. Correlations between MTFA and performance measures indicated that increases in MTFA lead to decreases in search time and decreases in fixation duration.

Accession For	
NTIS GRA&I	<input checked="" type="checkbox"/>
DDC TAB	<input type="checkbox"/>
Unannounced	
Justification	
By _____	
Distribution/	
Availability Codes	
Dist	Avail and/or special
A	

TABLE OF CONTENTS

	Page
I. INTRODUCTION	8
II. METHOD: DYNAMIC IMAGERY EXPERIMENT	12
EXPERIMENTAL DESIGN	12
APPARATUS	13
Variable Parameter Television System	13
Image Quality Manipulation	14
Stimuli	15
Stimulus Generation	17
Behavioral Data Acquisition System	18
PHOTOMETRIC MEASUREMENTS	18
SUBJECTS	22
PROCEDURE	22
III. RESULTS: DYNAMIC IMAGERY EXPERIMENT	27
TARGET ACQUISITION PERFORMANCE	27
EYE MOVEMENT DATA REDUCTION	35
EYE MOVEMENT PERFORMANCE	38
PHOTOMETRIC DATA REDUCTION	39
MTFA VALUES	41
MTFA-PERFORMANCE CORRELATIONS	44
IV. METHOD: STATIC IMAGERY EXPERIMENT	47
EXPERIMENTAL DESIGN	47
APPARATUS	48
Variable Parameter Television System	48
Image Quality Manipulation	49
Stimuli	49
Stimulus Generation	50
Behavioral Data Acquisition System	50
PHOTOMETRIC MEASUREMENTS	52
SUBJECTS	52
PROCEDURE	53
V. RESULTS: STATIC IMAGERY EXPERIMENT	56
TARGET ACQUISITION PERFORMANCE ANALYSIS	56

	Page
EYE MOVEMENT DATA REDUCTION	58
EYE MOVEMENT PERFORMANCE	59
PHOTOMETRIC DATA REDUCTION	60
MTFA-PERFORMANCE CORRELATIONS	61
 VI. DISCUSSION AND CONCLUSIONS	 67
TARGET ACQUISITION PERFORMANCE	67
MTFA UTILITY	67
EYE MOVEMENT RESULTS	69
 APPENDIX A: PROCEDURES USED TO ESTABLISH TRACK LOCK	 72
 APPENDIX B: DYNAMIC IMAGING SYSTEM MTF DATA	 82
 APPENDIX C: STATIC IMAGING SYSTEM MTF DATA	 85
 REFERENCES	 89

LIST OF TABLES

Table	Page
1. TARGET CHARACTERISTICS	16
2. SUMMARY OF ANALYSIS OF VARIANCE PERFORMED ON MEAN NUMBER OF CORRECT RESPONSES	28
3. SUMMARY OF ANALYSIS OF VARIANCE PERFORMED ON MEAN GROUND RANGE (FEET) FOR CORRECT RESPONSES	31
4. SUMMARY OF ANALYSIS OF VARIANCE PERFORMED ON MEAN GROUND RANGE, ZERO FEET SUBSTITUTED FOR INCORRECT RESPONSES	33
5. SUMMARY OF ANALYSIS OF VARIANCE PERFORMED ON MEAN GROUND RANGE, MINIMUM GROUND RANGE SUBSTITUTED FOR INCORRECT RESPONSES	35
6. SUMMARY OF ANALYSIS OF VARIANCE PERFORMED ON MEAN SACCADE DURATIONS	38
7. SUMMARY OF ANALYSIS OF VARIANCE PERFORMED ON MEAN FIXATION DURATIONS	39
8. MODEL OF MTF DATA: MODULATION AS A FUNCTION OF SPATIAL FREQUENCY (SF) IN CYCLES PER DEGREE	42
9. MODELS OF THRESHOLD DATA: MODULATION AS A FUNCTION OF SPATIAL FREQUENCY IN CYCLES PER DEGREE AND NOISE AMPLITUDE IN RMS mV	43
10. CALCULATED MTFAS FOR EACH COMBINATION OF SYSTEM AND NOISE LEVEL	44
11. CORRELATIONS BETWEEN MTFAS AND PERFORMANCE AND EYE MOVEMENT MEASURES	45
12. SUMMARY OF ANALYSIS OF VARIANCE PERFORMED ON MEAN NUMBER OF CORRECT RESPONSES	57
13. SUMMARY OF ANALYSIS OF VARIANCE PERFORMED ON MEAN SEARCH TIME	57
14. SUMMARY OF ANALYSIS OF VARIANCE PERFORMED ON MEAN FIXATION DURATION	60

Table	Page
15. SUMMARY OF ANALYSIS OF VARIANCE PERFORMED ON MEAN SACCADE DURATIONS	60
16. MODELS OF MTF DATA: MODULATION AS A FUNCTION OF SPATIAL FREQUENCY (SF) IN CYCLES PER DEGREE	62
17. CALCULATED MTFAS FOR EACH COMBINATION OF SYSTEM AND NOISE LEVEL	63
18. CORRELATIONS BETWEEN MTFA AND PERFORMANCE AND EYE MOVEMENT MEASURES	64

LIST OF ILLUSTRATIONS

Figure	Page
1. System MTFA Concept	9
2. Dynamic Imagery Experimental Design	12
3. Simplified Block Diagram of the Dynamic Imagery Video System	13
4. Simulated Flight Geometry	17
5. Simplified Block Diagram of Dynamic Imagery Eye Movement Data Acquisition System	19
6. Schematic of Photometer Connections	21
7. Dynamic Imagery Experiment: Percent Correct Responses as a Function of Noise Level	29
8. Dynamic Imagery Experiment: Percent Correct Responses as a Function of Target Size	29
9. Dynamic Imagery Experiment: Mean Correct Response Ground Range as a Function of Target Size	32
10. Dynamic Imagery Experiment: Mean Ground Range, Zero Feet Substituted for Incorrect Responses as a Function of System and Target Size	32
11. Dynamic Imagery Experiment: Mean Ground Range, with Minimum Ground Range Substituted for Incorrect Responses as a Function of System and Target Size	36
12. Dynamic Imagery Experiment: Mean Fixation Duration as a Function of Target Size	40
13. Static Imagery Experimental Design	47
14. Simplified Block Diagram of Static Imagery Video System	48
15. Simplified Block Diagram of Static Imagery Eye Movement and Behavioral Data Acquisition System	51

Figure	Page
16. Static Imagery Experiment: Mean Search Time as a Function of Noise Level and System	58
17. Static Imagery Experiment: Mean Fixation Duration as a Function of Noise Level and System	61
18. Diagram of Block Tri-Bar Showing Pattern Oriented Parallel to Raster Structure, Eyepiece Slit, and Direction of Scan	65

PREFACE

This study was initiated by the Visual Displays Branch, Human Engineering Division, of the Aerospace Medical Research Laboratory. The research was conducted by the Department of Industrial Engineering and Operations Research, Virginia Polytechnic Institute and State University, Blacksburg, Virginia 24061, under Air Force Contract F33615-76-C-5022. Dr. Harry L. Snyder was the Principal Investigator for Virginia Polytechnic Institute and State University. Mr. Wayne L. Martin and Dr. H. Lee Task were the Technical Monitors for the Aerospace Medical Research Laboratory. The report covers research performed between October 1975 and June 1977 under Task I: MTFA Evaluation.

I. INTRODUCTION

During the past eight years, considerable research emphasis has been placed upon the derivation and experimental evaluation of several unitary measures of image quality for raster-scan electronic displays. Such unitary measures, sometimes also called figures of merit, include the concepts of displayed signal-to-noise ratio (e.g., Rosell and Willson, 1973), noise equivalent bandwidth (e.g., Schade, 1973), optical power spectrum (Schindler and Martin, 1978), and modulation transfer function area (e.g., Snyder, 1973, 1976). In one form or another, each of these unitary measures takes into account the modulation transfer function (MTF) of the imaging system, which relates the displayed image modulation (contrast) to the input image modulation, as a function of spatial frequency.

One of the most studied measures of image quality, the modulation transfer function area (MTFA), makes use of the system MTF in conjunction with the threshold modulation function or detection threshold curve of the human visual system, as illustrated in figure 1. Briefly, the MTFA is the integral, over all usable spatial frequencies, of the modulation the imaging system can produce (the MTF) minus the modulation required by the visual system (threshold curve) for 50% detection of a sinusoidal grating.

Inherent in this concept is the isotropy of the MTFA. That is, equal increments *anywhere* in the shaded area of figure 1 are assumed to

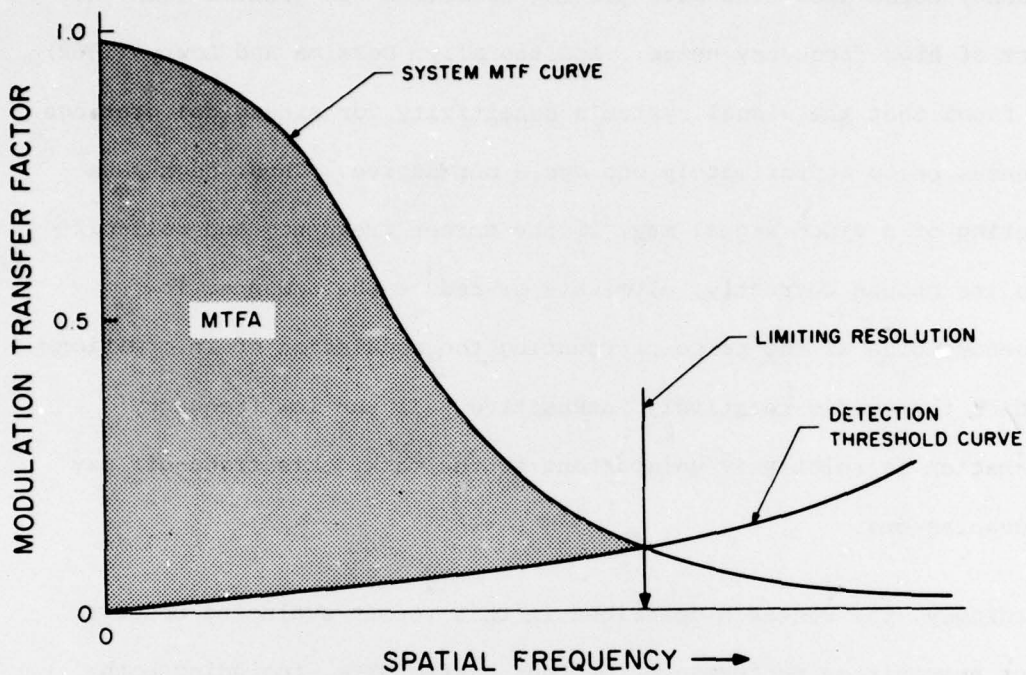


Figure 1. System MTF Concept.

produce equal increments in usable image quality. Thus, the concept does not distinguish between contributions to the MTF integral near the visual threshold versus well above threshold modulation. Further, it does not distinguish among contributions to the MTF made at various spatial frequencies, i.e.; it is not differentially sensitive to systems which have high-pass versus low-pass versus bandpass filtering, so long as the resultant MTF is constant.

While one can argue logically that the typical imaging system has a representative monotonically decreasing MTF and that a high-pass system is artificially contrived, there may be some advantages to a

high-pass filtered system. Keesee (1976) found that the effect of low frequency noise upon sine wave grating detection was greater than the effect of high frequency noise. Additionally, DePalma and Lowry (1962) have found that the visual system's sensitivity for sinusoidal gratings decreases below approximately one cycle per degree. Thus, high-pass filtering of a video signal may, if the corner frequency and roll-off slope are chosen correctly, eliminate or reduce the unwanted low frequency noise at the price of reducing the modulation of information to which the eye is relatively insensitive. If the low frequency information is relatively unimportant to the task, this trade-off may be advantageous.

Accordingly, the research described in this report evaluated observer target acquisition performance for four system MTFs, including both high-pass and low-pass filtered systems. MTFAs were calculated for all MTFs with three factorially combined noise levels to determine if the MTFA concept remained valid independent of the MTF shape; that is, the analysis determined whether the MTFA was isotropic.

Two experiments were performed, one with a static search field and one with dynamic air-to-ground imagery. For the static search experiment, the four systems included (1) a nonfiltered, nonattenuated system, (2) a nonfiltered system attenuated 7 dB over all spatial frequencies, (3) a low-pass filtered system, and (4) a high-pass filtered system. In the dynamic search experiment, preliminary studies indicated that the high-pass system was totally unusable because low spatial frequency information is necessary for target recognition. Thus, this experiment

evaluated only the first three system MTFs. Both experiments had three noise levels combined factorially with the different MTF shapes.

The secondary objective of these experiments was to evaluate the suitability and sensitivity of eye movement measurements as indices of image quality. In each experiment, continuous eye movement data were recorded from which were calculated both fixation durations and saccade durations. These eye movement measures were also related to the independent variables of system MTF, noise level, and the derived measure of MTFA.

II. METHOD: DYNAMIC IMAGERY EXPERIMENT

EXPERIMENTAL DESIGN

The experimental design of this study was a full factorial $3 \times 3 \times 3$ (System \times Noise Level \times Target Size) experiment. Target size was a within-subjects variable, while Noise Level and System were between-subjects variables. The experimental design is illustrated in figure 2.

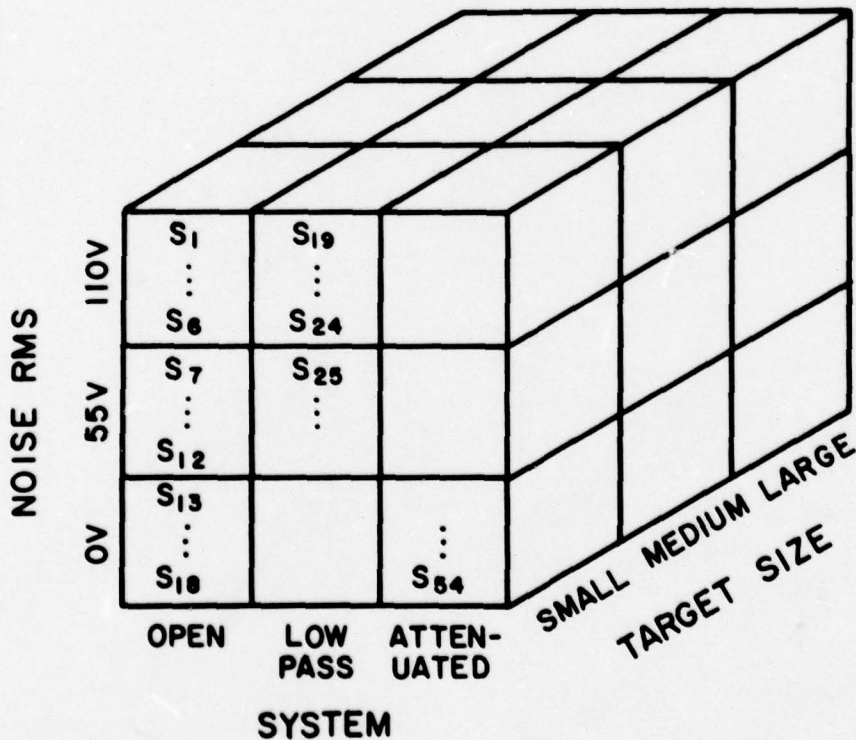


Figure 2. Dynamic Imagery Experimental Design

Each subject was presented with either an open system, a low-pass filtered system, or an attenuated system, and either 0 mV rms, 55 mV rms, or 110 mV rms noise added to the video signal. During the

course of the experiment, each subject viewed the same 35 mm film containing 17 targets, the first two of which were practice targets. The latter 15 targets were classified into three categories on the basis of ground size. This classification resulted in 5 small, 5 medium, and 5 large targets.

APPARATUS

Variable Parameter Television System

A simplified block diagram of the video system is presented in figure 3. The television camera, a Cohu Model 7000, was driven by a Cohu Model 6900 camera control unit at a line rate of 945 lines per frame. The frame rate was 30 frames per second, with a 2:1 positive interlace format.

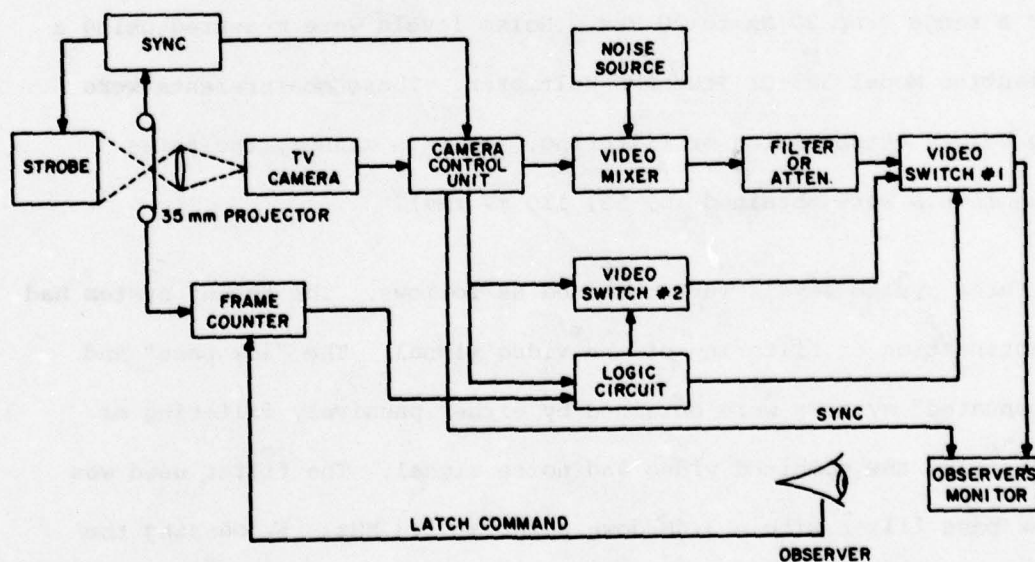


Figure 3. Simplified Block Diagram of the Dynamic Imagery Video System.

The observer's monitor, a Conrac Model QQA-17, measured 43 cm diagonally and had a P4 phosphor. The line rate of the monitor was set at 945 lines per frame, and the video signal sent to the monitor was altered in accordance with the experimental requirements. The TV camera and monitor were oriented so that the raster was vertical and the displayed picture had a 4:3 (vertical:horizontal) aspect ratio, in keeping with the format of the stimulus films.

Image Quality Manipulation

The quality of the image presented to the subject was manipulated in one of two ways. Electrical noise was added to the video signal by combining the output of a white noise generator with the camera control unit video signal in a custom designed, wideband video mixer. A General Radio Model 1383 Random Noise Generator provided white noise over a range from 20 Hz to 20 MHz. Noise levels were measured using a Ballantine Model 323-01 True RMS Voltmeter. These measurements were made before attenuation or filtering. In this manner, the three noise levels were obtained (0, 55, 110 mV rms).

The three system levels were obtained as follows. The "open" system had no attenuation or filtering of the video signal. The "low pass" and "attenuated" systems were obtained by either passively filtering or attenuating the combined video and noise signal. The filter used was a low pass filter with a 3 dB down point at 1.3 MHz. By passing the video signal, or the combined video and noise signal, through a Tektronix 2701 step attenuator, 7 dB of attenuation was obtained.

A specially designed video switch (labeled Video Switch 1 in figure 3) was interposed between the video mixer and the observer's monitor. This switch eliminated noise from that portion of the video signal used for monitor black level setting by switching to a noise-free blanking signal. This arrangement insured uniform black level setting by the observer's monitor. A logic circuit which sensed the onset of vertical and horizontal retrace controlled the signal which was passed to the observer's monitor. Whenever either of these retraces occurred, a noise-free signal was passed to the observer's monitor for the duration of the retrace. The addition of a second video switch (labeled Video Switch 2 in figure 3) permitted the selection of either of two blanking signal levels. This latter capability was used to control the luminance of the observer's monitor when blanked during presentation of briefing slides.

Stimuli

The imagery used during this experiment consisted of previously obtained 35 mm films of a 3000:1 terrain model located at the Columbus Division of North American Rockwell (Humes and Bauerschmidt, 1968). The film used in this study was photographed with a 35 mm film camera equipped with a 35 mm lens. This arrangement results in a 41° (horizontal) by 52.9° (vertical) field of view. The simulated flight geometry is illustrated in figure 4. The simulated flight altitude was 10,000 feet at a simulated velocity of 500 feet per second. The targets presented to the subjects are contained in table 1, which also contains the simulated ground dimension of each of the targets. (The first two targets were used only for practice.)

Table 1. TARGET CHARACTERISTICS

Target Number	Target Description	Target Length (ft)	Target Width (ft)	Target-Background Contrast
1	6 POL tanks	75	Diameter	0.647
2	SAM site	340	Diameter	0.414
3	6 small buildings	45	30	0.396
4	6 POL tanks	75	Diameter	0.647
5	6 POL tanks	75	Diameter	0.603
6	3 large buildings	70	60	0.559
7	4 MIGs	55	37	0.369
8	5 small buildings	40	30	0.133
9	4 small buildings	36	30	0.459
10	1 bridge & 3 boats	684	25	0.500
11	construction yard	1000	275	0.550
12	6 POL tanks	75	Diameter	0.505
13	SAM site	340	Diameter	0.324
14	4 small buildings	48	32	0.311
15	SAM site	340	Diameter	0.414
16	2 large buildings	120,70	60	0.482
17	Convoy of 8 missile vans	37	15	0.647

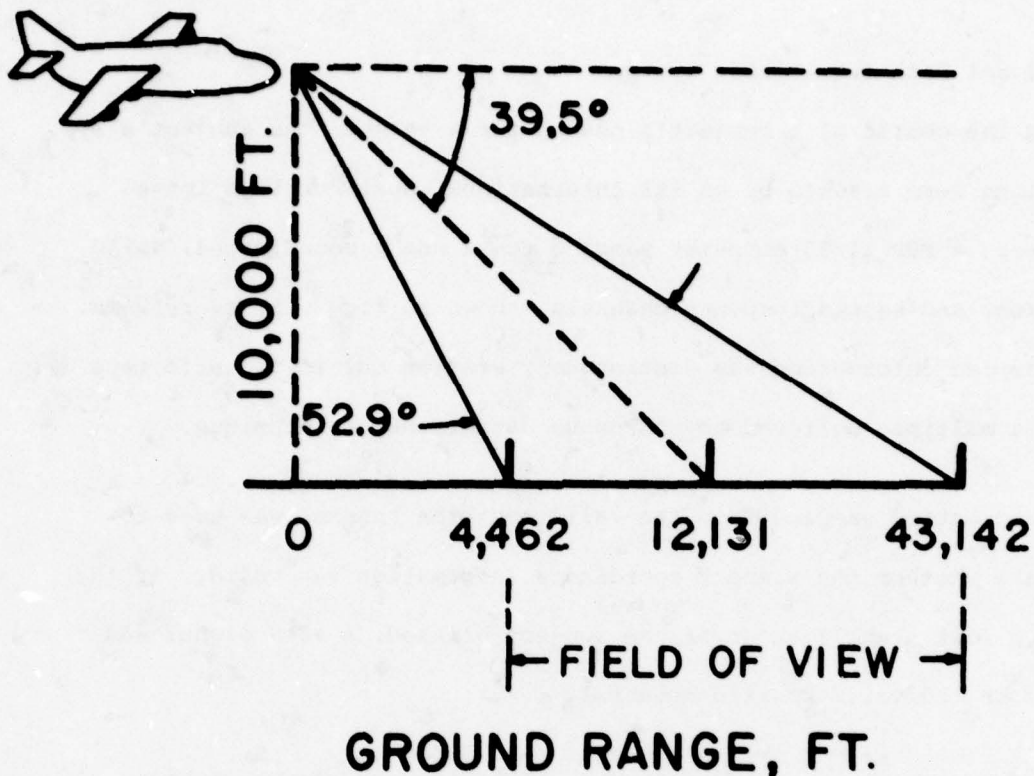


Figure 4. Simulated Flight Geometry

Stimulus Generation

A 35 mm Norelco motion picture projector, previously modified to provide synchronization to a television system (Humes and Bauerschmidt, 1968), was employed to focus the 35 mm imagery directly on the television camera vidicon photocathode. Modifications of this projector included deriving a frame pull-down synchronization signal from the flywheel of the projector, which permitted synchronization of the television system to the projector. Illumination of the film frame was achieved by synchronizing the discharge of a Strobex lamp to the film frame pull-down. The strobe was discharged at a rate of 60 flashes per second, or two flashes per TV frame. Thus, the camera saw only the stabilized image of the 35 mm film while the film frame was in the projector film gate.

Behavioral Data Acquisition System

During the course of a subject's search for a target, the subject's eye rotations were tracked by an SRI International Dual Purkinje image tracker. A PDP 11/55 computer sampled the x and y coordinates, valid position, and keypad response channels, shown in figure 5, every 2 ms. The sampled information was continuously written out to magnetic tape using a multiple buffered asynchronous data-transfer technique.

The information sampled from the valid position channel was used to indicate whether the x and y coordinate information was valid. If the tracker lost track lock or if the subject blinked, a +5 V signal was placed on the valid position channel.

Located on the right arm of the subject's chair was a seven-button keypad. Once the subject had visually acquired a target, the subject pressed a button. This button press latched a frame counter, and the frame count was recorded on a digital printer. In this way, the precise moment of the target acquisition response was recorded. The subject then indicated the location of the target on the television screen by pressing one of six buttons, each of which corresponded to an area encompassing one-sixth of the screen. These location response data were used to determine whether the subject had acquired the correct target.

PHOTOMETRIC MEASUREMENTS

All photometric measurements for this research were obtained using a Gamma Scientific Model 2400 Digital Photometer. Scanning across sections of the CRT was accomplished by having the PDP 11/55 computer engage and

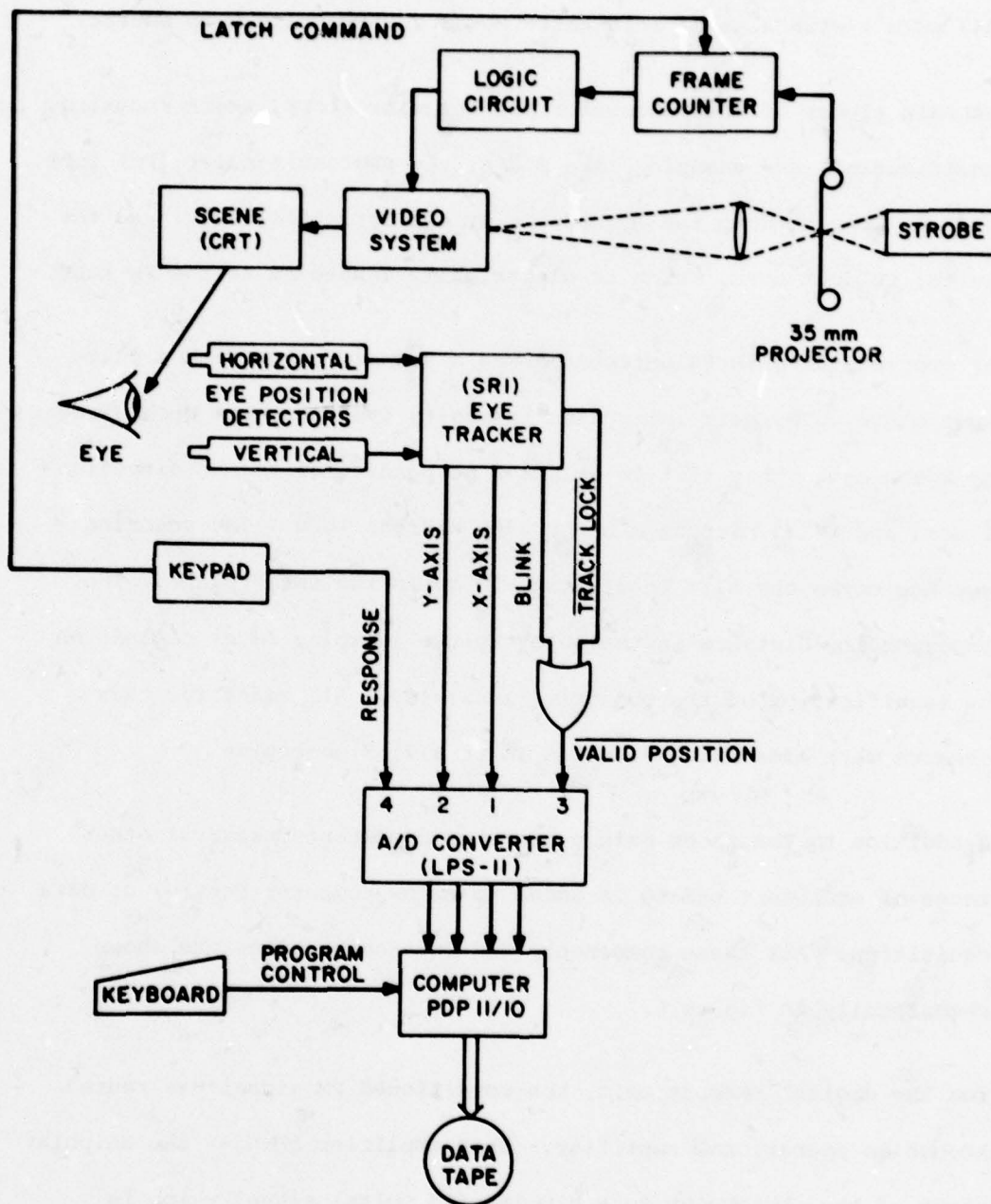


Figure 5. Simplified Block Diagram of the Dynamic Imagery Eye Movement Data Acquisition System.

disengage a scanning eyepiece drive made by Gamma Scientific. Prior to all measurements, the photometer was calibrated to 100 foot-Lamberts (343 cd/m^2) with a Gamma Scientific Model 220 Standard Lamp Source.

The main pieces of the photometer are the microscope, where focusing, magnification, and scanning take place; the photomultiplier (PM) tube, which is connected to the microscope by a fiber optic cable; and the digital readout unit, which is electrically connected to the PM tube.

The eyepiece used in this research was a scanning type with a slit input stage. The slit integrates intensity over its area much as does the human eye. This slit is oriented perpendicular to the direction of scan and is 25 microns wide by 2500 microns long. The scanning eyepiece moves the slit input stage 10 mm in the image plane. The corresponding distance in the object plane (display face) depends on the magnification of the objective lens used. All scans for this research were made using either a 1X or a 2.5X objective.

In addition to the three main photometer components, several other pieces of equipment had to be added to allow computer control of data acquisition. All these components and interconnections are shown schematically in figure 6.

From the digital readout unit, the conditioned PM signal was routed through an operational amplifier. This amplifier changes the unipolar output of the photometer to a bipolar (± 5 volts) signal which is compatible with the analog/digital front end (LPS-11) of the computer. A power supply was used in place of batteries for the scanning motor.

This power supply voltage was routed through a relay which was controlled by the computer. A voltage was also taken from this power supply to signal the computer program that a scan should be taken.

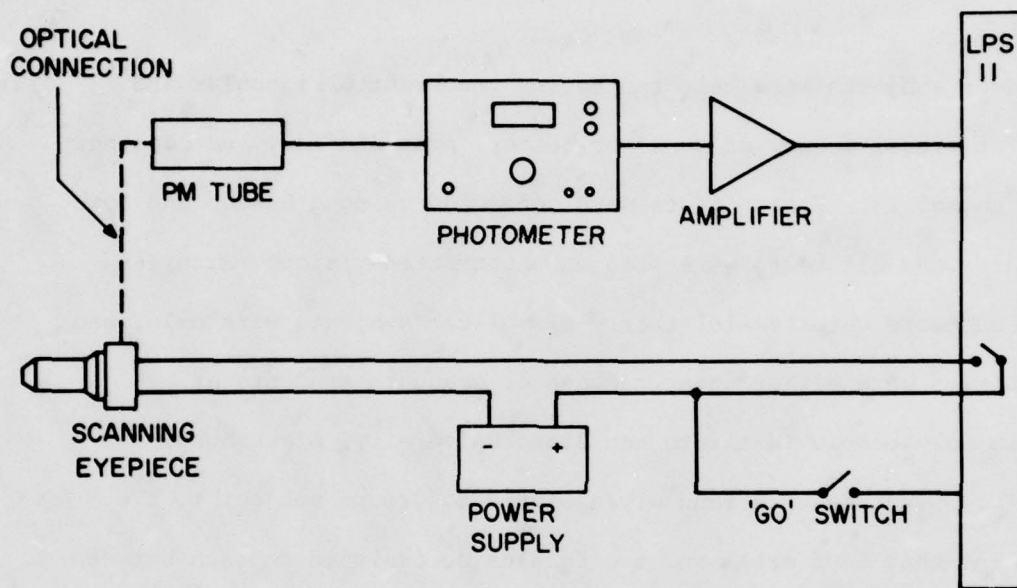


Figure 6. Schematic of Photometer Connections

When a "go" signal was sent to the computer, the scanning drive relay was closed for exactly 60 s. The voltage of the power supply was set so that the scanning slit traversed 10 ± 0.05 mm along the image plane in that 60-s period, during which the analog/digital front end of the computer was sampling the output of the photometer (through the operational amplifier). The sampling rate was once every 10 ms, and the data were stored on magnetic tape. At the end of a scan, a file containing 6000 data points taken at equally spaced intervals in time and space existed on magnetic tape. Such a scan was taken both vertically and

horizontally across standard 1951 USAF tri-bar patterns (square wave intensity variation) displayed at the monitor. The displayed patterns were obtained by placing the tri-bar patterns in the film gate of the 35 mm film projector and operating the video system as described above.

SUBJECTS

Fifty-four subjects were selected having uncorrected binocular and monocular visual acuity of 20/20 or better, near and far, and no other visual anomalies. Vision tests were conducted using a Bausch and Lomb Orthorater and all tests were made on uncorrected vision. Eighteen of the subjects were female, thirty-six of the subjects were male, and all subjects were either undergraduate or graduate students at Virginia Polytechnic Institute and State University, Blacksburg, Virginia. Subjects were randomly assigned to groups subject to the constraint that four males and two females be assigned to each between-subjects group. All subjects were volunteers, and they were paid \$2.50 per hour for their participation.

PROCEDURE

Each subject participated in a preexperiment session. The purpose of this session was to insure that the eye tracker could maintain track lock over a field of view corresponding to the size of the observer's monitor. The first part of each session involved explaining, in general terms, the purpose of the experiment and the operating procedure of the eyetracker.

The second part of each preexperimental session was taken up with establishing track lock. First, a bite bar was made for each subject.

This bite bar consisted of a "U" shaped piece of metal upon which dental wax was molded. A partial dental impression was made by heating the wax on the bite bar and then having the subject bite down on the bar.

After the impression was made and the wax had hardened, the bite bar was placed in a holder, which was attached to a modified machinist's stage which moved vertically, horizontally, and axially. The subject was seated in a chair equipped with a hydraulic lift. This enabled the experimenter to position the bite bar and then to move the subject to the bite bar.

The subject viewed a 3×3 matrix of red LEDs placed on a gray board at a distance of 102 cm from the subject. The LEDs were separated vertically by 11.4 cm and horizontally by 10.8 cm. The subject was instructed to fixate at the center of the matrix while track lock was established. The procedure used to establish track lock is contained in Appendix A. Once track lock was established, the subject was instructed to separately fixate each LED in the matrix. In some cases, due to small pupil size, or due to imaging of the subject's eyelashes in the tracker's optical path, track lock could not be maintained over the matrix. In such cases, the subject was paid for his/her time and dismissed. If track lock was stable as the subject scanned the matrix, the bite bar coordinates were noted and a session for the main experiment was scheduled.

Before the subject arrived for the experimental session, the video system was calibrated and the stimulus film was mounted. Video system calibration consisted of placing a gray scale of known characteristics

in the film gate of the 35 mm projector. Using an oscilloscope, synchronized to the line rate of the video system, the camera control unit was adjusted to produce a predetermined video signal amplitude. These adjustments were achieved by varying the gain of the camera control unit and the blanking signal level. Having assured that the correct signal was being sent to the observer's monitor, the monitor's "brightness" and "contrast" controls were set to yield a picture of the gray scale with predetermined luminances. These area luminances were monitored using a Minolta "Auto Spot II" light meter.

Upon arrival, each subject was read a description of the experiment and given a book containing enlarged photographs of the targets he/she would be asked to find. Each subject was informed that the purpose of the experiment was to assess the effects of image quality on eye movements and that the subject's task during the course of the experiment was to press a button as soon as he/she could positively identify the target. Each subject was familiarized with the configuration of the keypad used for responding.

After the subject had examined the target book and had become familiar with the configuration and sequence of the targets, the subject was led back to the area where the eye tracker was located. Track lock was established, and the stability of track lock was assessed by having the subject fixate on each of the LEDs presented during the preexperimental session. Before beginning the experiment, the subject was asked to voice any questions concerning the experiment or his/her task.

The room illuminance was kept at 20 lux throughout the experiment, and the observer's monitor was placed 101.6 cm away from the subject. Each

subject was asked to locate each of the 17 targets. For the five seconds immediately before each target came into view, the subject's monitor was blanked, and a slide of the upcoming target was projected onto the subject's monitor. The slide of the target was the same as the photograph of the target presented to the subject before the start of the experiment. These slides and photographs were enlargements of the targets to be located, but were cropped to include only the target and none of the surrounding area. After the 5-s presentation, the picture of the film was returned to the observer's monitor. (This "cueing" of the target's occurrence did not bias the subject's performance because targets were well below threshold detection levels when they first entered the displayed field of view.)

The presentation of the briefing slide was controlled by an event counter. The event counter input consisted of the film frame counts. When the number of frames counted equaled a preset value, a toggle switch would change state. This change of state was used to control a video switch which switched between a pure blanking signal and the normal video and blanking signal. In this way the screen could be blanked for presentation of the briefing slide, and this presentation occurred just before the target actually came into the displayed field of view.

After the briefing slide was turned off and the picture of the film was restored, the subject began to search for the target. Upon acquiring the target, the subject was instructed to press a button. This button press latched the frame counter output and printed that result. Having indicated target acquisition, the subject next indicated in which sixth

of the screen the target was located. This was signalled by pressing one of six buttons corresponding to areas formed by dividing the screen in half in the vertical axis and into thirds along the horizontal axis of the observer's monitor. No visual aids were given to the subject to indicate the screen divisions. The subject was instructed to make the best estimation possible.

Twelve targets were presented to the subject on the first of two films, and the remaining five targets were presented on a second film. During the film change, the subject was given a 5-min break. During the break, the subject remained seated in the experimental area but was not required to remain on the bite bar. Following the loading of the second film, track lock was reestablished and then the film was started.

III. RESULTS: DYNAMIC IMAGERY EXPERIMENT

TARGET ACQUISITION PERFORMANCE

Each subject's response to each target was judged as either correct or incorrect. Correctness was determined by comparing target location as indicated by the subject with the expected location of the target on the display at the time of response. The expected target location was determined by extrapolating between the target position on the first and last frames during which the target was on display, and on the basis of the film frame number indicated at target acquisition. If a target passed through the intersection of two adjacent areas at the time of the subject's response, a response to either area was counted as correct. Trials during which the subject failed to acquire the target were counted as incorrect.

A $3 \times 3 \times 3$ analysis of variance (System \times Noise Level \times Target Size) was performed on the mean number of correct responses. The mean number of correct responses was obtained by summing the number of correct responses across subjects and targets in the same System and Noise Level conditions for each target size. The results of the analysis are presented in table 2, which shows that the main effects of Noise Level ($p < 0.054$), and Target Size ($p < 0.001$) were significant.

Figure 7 portrays the effect of Noise Level on the number of correct target acquisitions expressed as percent correct. Newman-Keuls tests performed on the mean number of correct responses for each Noise Level

Table 2. SUMMARY OF ANALYSIS OF VARIANCE PERFORMED ON MEAN NUMBER OF CORRECT RESPONSES

Source of Variance	SS	df	MS	F	p
System (Sys)	34.67	2	17.34	2.99	> 0.10
Noise Level (NL)	49.55	2	24.78	4.27	< 0.06
Sys × NL	27.78	4	6.95	1.20	> 0.10
Target Size (Size)	1974.89	2	987.45	170.09	< 0.0001
Sys × Size	9.78	4	2.45	0.42	> 0.10
NL × Size	15.55	4	3.89	0.67	> 0.10
Sys × NL × Size	46.44	8	5.81	----	----

indicated no significant differences between the 0 mV rms and 55 mV rms noise groups ($p > 0.10$) and that each of these groups yielded higher numbers of correct responses than the 110 mV rms group ($p < 0.10$).

Newman-Keuls tests on the Target Size mean number correct scores revealed significant differences among all three means ($p < 0.001$). As can be seen from figure 8, large-sized targets resulted in the highest percent of correct responses, followed by medium-sized and then by small-sized targets.

Ground range was calculated from film frame number at target acquisition using the following equation:

$$\text{GROUND RANGE} = R_{\text{max}} - [(F_{\text{resp}} - F_{\text{max}}) \times \text{FR}] , \quad (1)$$

where

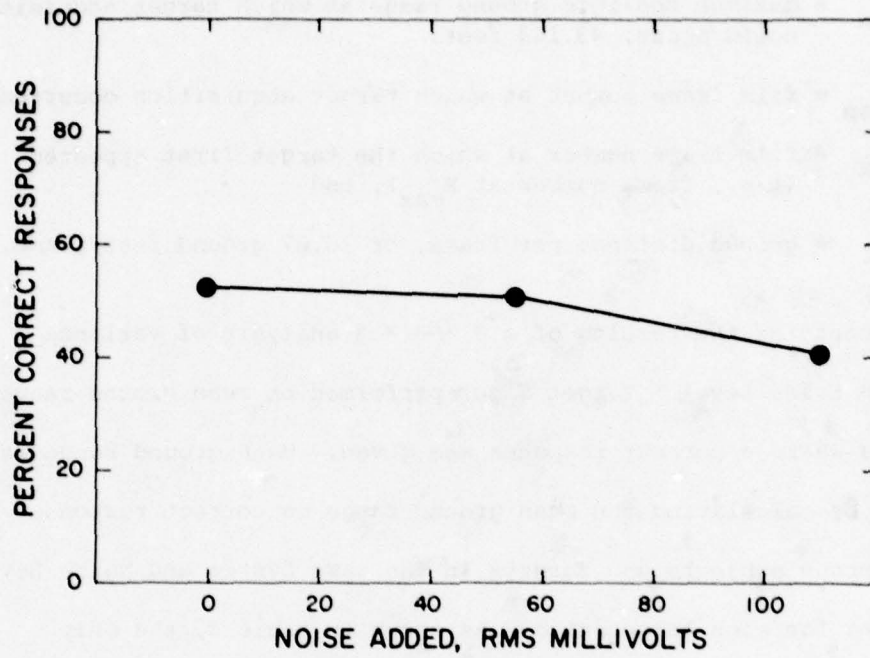


Figure 7. Dynamic Imagery Experiment: Percent Correct Responses as a Function of Noise Level.

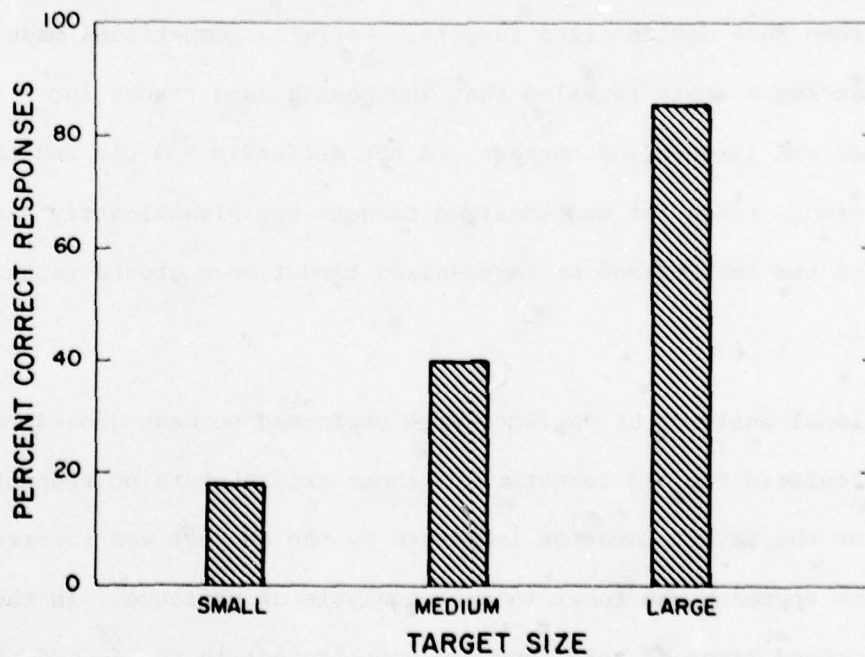


Figure 8. Dynamic Imagery Experiment: Percent Correct Responses as a Function of Target Size.

- R_{\max} = maximum possible ground range at which target acquisition could occur, 43,143 feet,
- F_{resp} = film frame number at which target acquisition occurred,
- F_{\max} = film frame number at which the target first appeared (i.e., frame number at R_{\max}), and
- FR = ground distance per frame, or 16.67 ground feet/frame.

Table 3 contains the results of a $3 \times 3 \times 3$ analysis of variance (System \times Noise Level \times Target Size) performed on mean ground range on trials where a correct response was given. Mean ground range was obtained by calculating the mean ground range on correct response trials across subjects and targets in the same System and Noise Level conditions for each target size. As shown in table 3, the only significant effect was Target Size. As can be seen in figure 9, small-sized and large-sized targets were correctly identified at a greater distance than were medium-sized targets. Pairwise comparisons made with Newman-Keuls tests revealed that the mean ground ranges for small-sized and large-sized targets did not differ ($p > 0.05$) and that the mean ground range for medium-sized targets was significantly smaller than either the small-sized or large-sized target mean ground range ($p < 0.01$).

Two additional analyses of variance were performed on mean ground range scores calculated for all targets. On those trials where no response was made or the target location indicated by the subject was incorrect, a different approach was taken in each analysis of variance. In the first, a ground range of zero feet was substituted; in the second, the minimum possible target range of 4,463 feet was substituted.

Table 3. SUMMARY OF ANALYSIS OF VARIANCE PERFORMED ON MEAN GROUND RANGE (FEET) FOR CORRECT RESPONSES

Source of Variance	SS	df	MS	F	p
System (Sys)	8664261.51	2	4332130.75	0.66	> 0.10
Noise Level (NL)	23589457.78	2	11794728.89	1.79	> 0.10
Sys × NL	43819377.78	4	10954844.45	1.66	> 0.10
Target Size (Size)	294002219.85	2	148501109.43	22.31	< 0.001
Sys × Size	47061272.54	4	11765318.14	1.79	> 0.10
NL × Size	38525468.10	4	9631367.03	1.46	> 0.10
Sys × NL × Size	52723441.07	8	6590430.13	----	----

The substitution of zero range or minimum range for ground range on those trials where incorrect responses were made has several advantages. One advantage is that the substitution results in an equal number of scores per cell of the design without, as in the previous analysis, the necessity of obtaining mean ground ranges across subjects. Thus, an F-ratio denominator was obtained for the System × Noise Level × Target Size interaction and the perils of unequal-n analysis of variance were avoided. The second advantage is that the substitutions reduce the mean ground range by some amount related to the likelihood of making errors. The substitution of zero range imposes a larger penalty for incorrect responses than the substitution of the minimum ground range. Previous studies (Bonnett, 1975; Snyder, 1976) have demonstrated the meaningfulness of these substitutions.

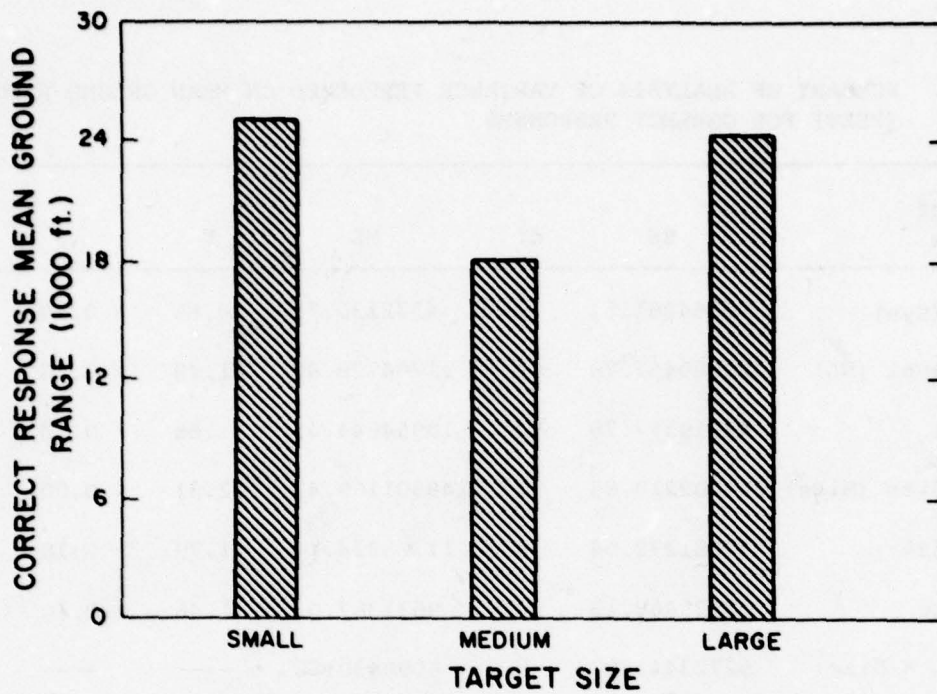


Figure 9. Dynamic Imagery Experiment: Mean Correct Response Ground Range as a Function of Target Size

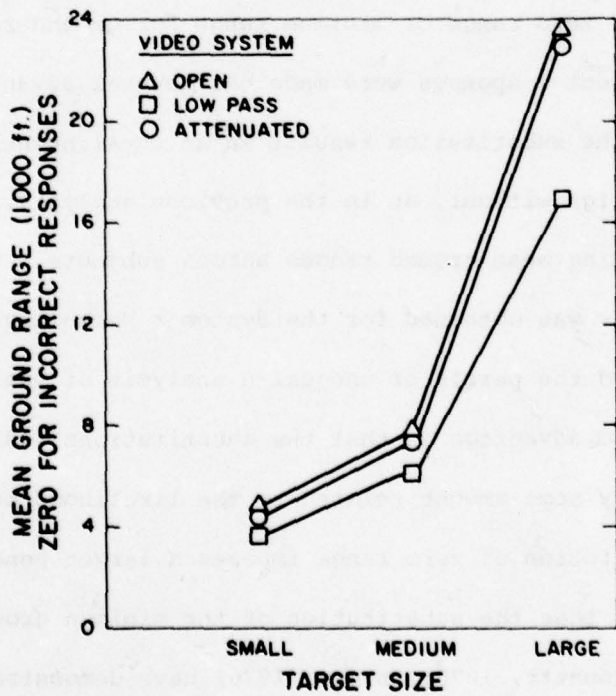


Figure 10. Dynamic Imagery Experiment: Mean Ground Range, Zero Feet Substituted for Incorrect Responses as a Function of System and Target Size

The first of these analyses, a $3 \times 3 \times 3$ analysis of variance (System \times Noise Level \times Target Size), was performed on mean ground range scores calculated with a ground range of zero substituted for incorrect response trial ground range. The results of the analysis, presented in table 4, indicate significant effects due to System ($p < 0.017$), Target Size ($p < 0.001$), and the System \times Target Size interaction ($p < 0.05$).

Table 4. SUMMARY OF ANALYSIS OF VARIANCE PERFORMED ON MEAN GROUND RANGE, ZERO FEET SUBSTITUTED FOR INCORRECT RESPONSES

Source of Variance	SS	df	MS	F	p
System (Sys)	308276404.3	2	154138202.2	4.46	0.017
Noise Level (NL)	106264839.1	2	53132419.5	1.54	> 0.10
Sys \times NL	136093204.1	4	3402330.0	0.98	> 0.10
S/Sys,NL	1556538968.1	45	34589532.6	-----	-----
Target Size(Size)	8437493716.1	2	42187468.6	206.57	< 0.001
NL \times Size	117005446.2	4	29251361.5	1.43	> 0.10
Sys \times Size	201694952.4	4	50423738.1	2.47	0.05
Sys \times NL \times Size	85388822.4	8	10673602.8	0.52	> 0.10
Size \times S/Sys,NL	1838027473.8	90	20422527.5	-----	-----

The System \times Target Size interaction is graphically represented in figure 10, which shows that the large-sized target mean ground range was generally larger than either the medium-sized or small-sized target mean ground ranges. In addition, the effect of System is most

pronounced for the large targets. In particular, the open and attenuated systems yielded larger ground ranges than the low-pass filtered system. Further analyses with Newman-Keuls tests revealed that mean ground ranges did not differ as a function of System for either the small or the medium target sizes ($ps > 0.05$). Similarly, the mean ground ranges for each system did not differ between the small- and medium-sized targets ($ps > 0.05$). Large target mean ground ranges were significantly larger than small- or medium-sized target mean ground ranges for all levels of the System variable ($ps < 0.05$). Mean ground ranges for large-sized targets were not significantly different for the open and attenuated conditions, and both of these mean ground ranges were significantly larger than the large-sized target low-pass filtered system mean ground ranges.

The $3 \times 3 \times 3$ analysis of variance (System \times Noise Level \times Target Size) performed on mean ground range scores with a ground range of 4,463 ft substituted for incorrect response trial ground range revealed a main effect of System ($p = 0.013$), a main effect of Target Size ($p < 0.001$), and a significant System \times Target Size interaction ($p < 0.021$). As shown in figure 11, the source of the interaction was again the differential effect of System which appears for the large targets. Newman-Keuls tests revealed that for the small-sized and medium-sized targets, mean ground ranges did not differ as a function of System, nor did the mean ground ranges for each system differ between the small-sized and medium-sized targets, $ps > 0.05$. Large-sized target mean ground ranges were significantly longer than small-sized or medium-sized target mean ground ranges for all levels of the System variable

($p_s < 0.05$). For the large-sized targets, the low-pass filtered system yielded shorter mean ground ranges than either the open or attenuated systems, $p_s < 0.05$. The mean ground ranges for large-sized targets for the open and attenuated systems did not differ, $p_s > 0.05$.

Table 5. SUMMARY OF ANALYSIS OF VARIANCE PERFORMED ON MEAN GROUND RANGE, MINIMUM GROUND RANGE SUBSTITUTED FOR INCORRECT RESPONSES

Source of Variance	SS	df	MS	F	p
System (Sys)	237844761.0	2	118922380.5	4.82	0.013
Noise Level (NL)	60234851.1	2	30117425.5	1.22	> 0.10
Sys × NL	97261549.9	4	24315387.5	0.99	> 0.10
S/Sys,NL	1109634363.6	45	24658541.4	----	----
Target Size(Size)	5767991938.1	2	288399596.5	200.70	< 0.001
NL × Size	92705681.1	4	23176420.3	1.61	> 0.10
Sys × Size	175390222.4	4	43847555.6	3.05	0.021
Sys × NL × Size	50913656.4	8	6364207.1	0.44	> 0.10
Size × S/Sys,NL	1293247987.2	90	1436942.2	----	----

EYE MOVEMENT DATA REDUCTION

As described in Evans and Gutmann (1978), the first step in the eye movement data reduction process consisted of estimating the instantaneous velocity and acceleration in the vertical (Y) and horizontal (X) dimensions. Derivatives of eye position were obtained using a derivative calculation technique which convolves an integer list with a vector of

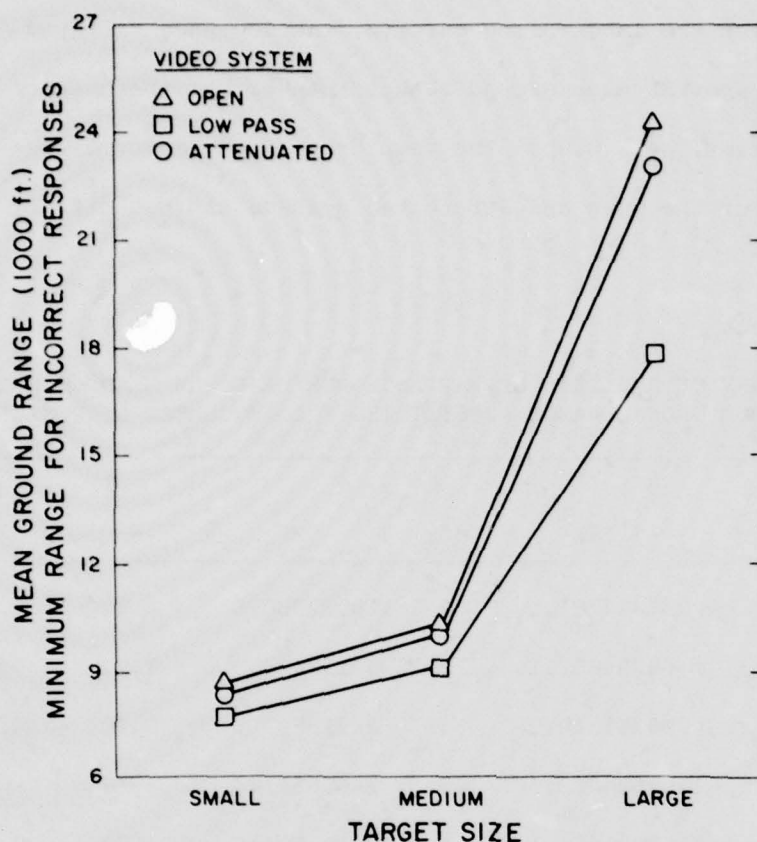


Figure 11. Dynamic Imagery Experiment: Mean Ground Range, with Minimum Ground Range Substituted for Incorrect Responses as a Function of System and Target Size

raw data. The resulting derivative estimate is the least-squares fit for the polynomial chosen (Hershey, Zaking, and Simha, 1967; Savitsky and Golay, 1964; Steiner, Termonia, and Deltour, 1972). By using a sliding vector of raw data points, derivative estimates may be calculated for each data point rather than only at the center points of vectors that are disjoint in time. Another advantage is that the derivative estimates produce little noise as compared to difference calculations.

The magnitude of the velocity vector, $(\dot{X}^2 + \dot{Y}^2)^{1/2}$, and the magnitude of the acceleration vector, $(\ddot{X}^2 + \ddot{Y}^2)^{1/2}$, were calculated for each data point and stored in a ring buffer. The sum of the velocity and acceleration magnitudes stored in each sliding vector served as the basis of classification. If the velocity and acceleration sums each exceeded specified threshold values, then a classification of saccade was made for the original X and Y data points associated with the midpoint of the velocity and acceleration sliding vector. If either of the sums was less than its respective threshold value, then a classification of fixation was made. Thus, high velocity and acceleration eye movements resulted in a classification of saccade, while lower velocity and acceleration movements resulted in a classification of fixation.

With the exception of the few points initially needed to fill the sliding vectors and a few points at the end of each trial, a classification was made for each X-Y pair of data points. Thus, classifications were made for each 2 ms of search. Event durations are determined by summing the number of sequential classifications of the same type and multiplying this sum by the reciprocal of the sampling rate. Mean fixation and mean saccade durations were calculated for each target. If, during the course of a subject's search, track lock was not established, then mean durations of zero were reported. The threshold values used as the basis of classifications were determined empirically. The values were chosen so as to minimize the number of fixation durations less than 20 ms and the number of saccade durations less than 10 ms. The same threshold values were used for all subjects. A discussion of

the classification parameters and values used is contained in Evans and Gutmann (1979).

EYE MOVEMENT PERFORMANCE

Analyses of variance were performed on mean fixation durations and mean saccade durations. Mean durations for each target size were calculated by taking the mean of the non-zero durations obtained for each target within a target size.

The results of a $3 \times 3 \times 3$ (Systems \times Noise Level \times Target Size) analysis of variance performed on mean saccade durations are contained in table 6. As can be seen from this table, none of the main effects or interactions were significant ($p > 0.10$).

Table 6. SUMMARY OF ANALYSIS OF VARIANCE PERFORMED ON MEAN SACCADE DURATIONS

Source of Variance	SS	df	MS	F*
System (Sys)	385.70	2	192.85	1.14
Noise Level (NL)	247.65	2	123.83	0.73
Sys \times NL	769.12	4	197.28	1.13
S/Sys,NL	7634.74	45	169.66	----
Target Size (Size)	7.55	2	3.78	0.06
Sys \times Size	268.67	4	67.17	1.02
NL \times Size	190.09	4	47.52	0.72
Sys \times NL \times Size	575.59	8	71.95	1.10
Size \times S/Sys,NL	5904.48	90	65.61	----

*All $p > 0.10$.

Table 7 contains the results of an analysis of variance performed on mean fixation durations. The only significant effect was that of Target Size. Mean fixation durations as a function of Target Size are shown in figure 12. Newman-Keuls tests among the mean fixation durations for each target size revealed that the large-sized targets yielded longer durations than either the small-sized or medium-sized targets ($p < 0.01$) and that durations associated with the small- and medium-sized targets did not differ from each other ($p > 0.01$).

Table 7. SUMMARY OF ANALYSIS OF VARIANCE PERFORMED ON MEAN FIXATION DURATIONS

Source of Variance	SS	df	MS	F	p
System (Sys)	77596.86	2	38798.43	1.46	> 0.10
Noise Level (NL)	50971.89	2	25485.95	0.96	> 0.10
Sys × NL	127647.58	4	31911.90	1.20	> 0.10
S/Sys,NL	1192340.55	45	26496.46	-----	-----
Target Size (Size)	196839.72	2	98419.86	22.72	< 0.001
Sys × Size	6785.06	4	1686.27	0.39	> 0.10
NL × Size	9484.53	4	2371.12	0.55	> 0.10
Sys × NL × Size	43075.64	8	5384.46	1.24	> 0.10
Size × S/Sys,NL	389914.98	90	4332.39	-----	-----

PHOTOMETRIC DATA REDUCTION

It was noted previously that the displayed image was scanned photometrically using a 1951 USAF tri-bar pattern as the optical input to

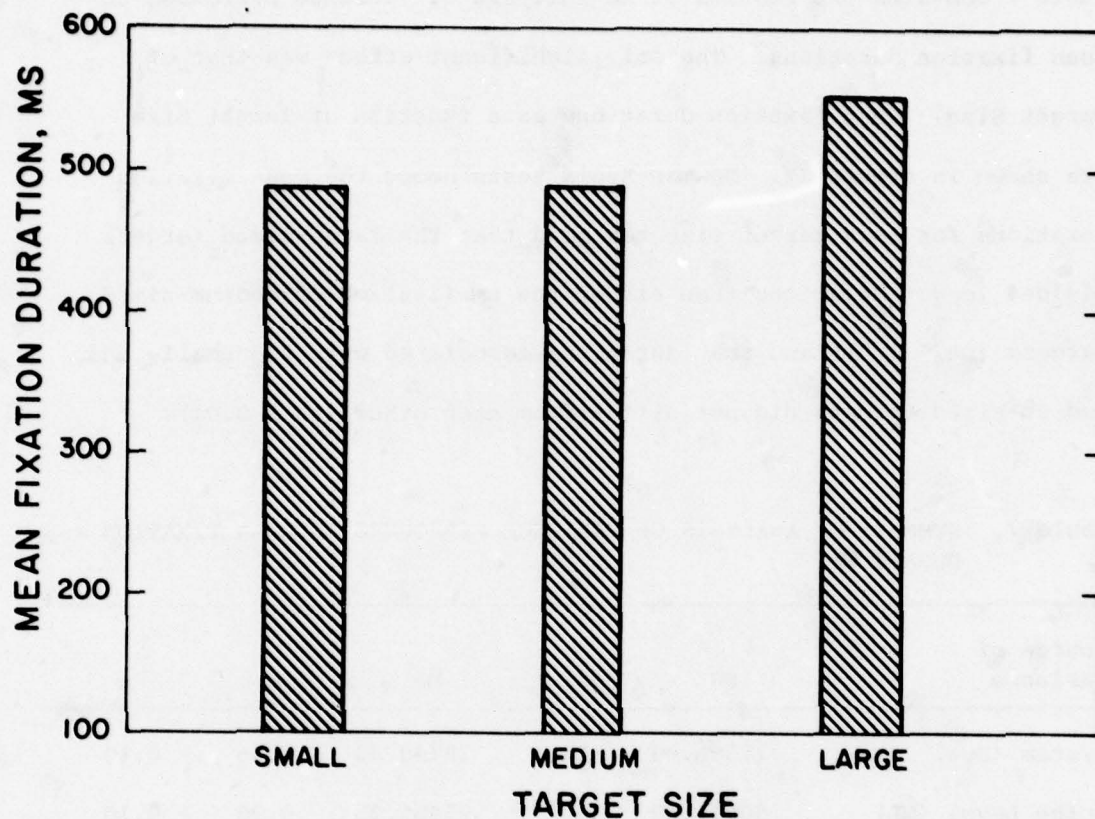


Figure 12. Dynamic Imagery Experiment: Mean Fixation Duration as a Function of Target Size.

the TV system. The photometric scans described previously produce files on magnetic tape which contain luminance values at certain discrete points on the display. The method used to analyze the spatial frequency content of these scans was numerical Fourier analysis. The IBM routine FORIT was used to calculate a given number of Fourier coefficients for any scan. This routine assumes that the input to it is a tabulated periodic function with an integral number of cycles in an array. The requirement of integral cycle input mandated the use of an optimization routine to select the correct number of points as input to FORIT.

The optimization routine used in this research (Maddox, 1977) was necessary because few, if any, actual photometric scans contained an exact integral number of cycles of the tri-bar pattern. It was not practical, due to the amount of time required, to simply delete one point at a time until an integral cycle point was located.

The criterion used for search direction reversals was the modulation of the fundamental spatial frequency of interest. It has been shown that the modulation of any spatial frequency can be calculated as the power at that frequency divided by the average intensity of the scan (Keesee, 1976). There are two assumptions made in this optimizing routine. First, at least one cycle of the function must be present in the scan. This is necessary because the search routine can only eliminate points from the scan, not add points to it. If less than one cycle were present, it is probable that the routine in its present form would attempt to optimize at zero cycles. Second, the optimization procedure assumes that a local maximum is also the global maximum. This assumption is met by the nature of the Fourier analysis routine, i.e., the power of a given frequency has only one maximum in the neighborhood of an integral number of cycles of that frequency.

Once the scan data were trimmed to the appropriate number of points, the modulation of the fundamental was calculated. This procedure provided, for each scan, the fundamental spatial frequency and its associated modulation. These data are contained in Appendix B.

MTFA VALUES

In order to calculate MTFAs, as stated previously, the system MTF and observer threshold curves must be determined. An expression of each

system's MTF curve was obtained by fitting a quadratic model to the spatial frequency-modulation data obtained for each system. The coefficients for each model were estimated using a multiple regression fit, the results of which are contained in Table 8. The MTF versus spatial frequency data for each system are contained in Appendix B.

Table 8. MODEL OF MTF DATA: MODULATION AS A FUNCTION OF SPATIAL FREQUENCY (SF) IN CYCLES PER DEGREE

System	R^2	Modulation = Intercept	+	$(SF)^2$
<i>Targets Perpendicular to the Raster:</i>				
Open (O)	0.74	0.7870264		-.00468442
Attenuated (A)	0.96	0.5152346		-.00321165
Low Pass (LP) Filtered	0.48	0.31491202		-.00218117
<i>Targets Parallel to the Raster:</i>				
O	0.92	0.84758123		-.00271652
A	0.60	0.77470292		-.00327522
LP	0.86	0.77470292		-.00280551

Keesee (1976) has collected the data needed to estimate modulation detectability thresholds for sinusoidally varied luminance gratings presented on medium to high resolution black and white television monitors in the presence of electrical noise added to the video signal. The threshold data collected by Keesee for a 945-line system are the most relevant to the present study. Of the different noise pass bands used by Keesee, the 0-16 MHz condition was the most like the noise conditions of the present study.

The threshold data obtained by Keesee were used to model the relative effects of added noise on detection thresholds. The absolute effects of added noise on detection thresholds cannot be derived from Keesee's data because the levels of added noise used in Keesee's experiment and the experiments reported here cannot be directly equated. Due to differences in the displays and the video system, it is not possible to relate input noise amplitude to displayed luminance across experiments. Keesee's data do provide, however, an empirical basis for predicting the relative effects of added noise on detection thresholds.

An expression for the threshold curves was obtained by fitting a second order polynomial model to the mean detectable modulation-spatial frequency data obtained by Keesee. Multiple regression fits were used to estimate the model coefficients which are contained in table 9. Two equations, one for targets parallel to the raster structure and one for targets perpendicular to the raster structure, were obtained.

Table 9. MODELS OF THRESHOLD DATA: MODULATION AS A FUNCTION OF SPATIAL FREQUENCY IN CYCLES PER DEGREE AND NOISE AMPLITUDE IN RMS mV

R ²	Modulation =						
	(SF) ²	+	(NA) (SF)	+	(SF)	+	Intercept
<i>Targets Perpendicular to the Raster:</i>							
0.94	0.00004989		0.00006555		-0.00014445		0.00729351
<i>Targets Parallel to the Raster:</i>							
0.62	0.00012973		0.0000649		-0.00246575		0.01817905

MTFAs, for targets either perpendicular or parallel to the raster, were obtained by solving:

$$MTFA = \int_0^i [F_1(SF) - F_2(SF)] d(SF) , \quad (2)$$

where

$F_1(SF)$ = MTF equation,

$F_2(SF)$ = threshold equation,

SF = spatial frequency in cycles per degree, and

i = intersection of the MTF and threshold curves.

The results of the MTFA calculations are contained in table 10.

Table 10. CALCULATED MTFAS FOR EACH COMBINATION OF SYSTEM AND NOISE LEVEL

System	Noise Level		
	0 mV	55 mV	110 mV
<i>Targets Perpendicular to the Raster:</i>			
Open (O)	6.6854	6.3962	6.1238
Attenuated (A)	4.2387	3.9688	3.7219
Low Pass Filtered (LP)	2.4185	2.1848	1.9811
<i>Targets Parallel to the Raster:</i>			
Open (O)	9.8076	9.2800	8.7898
Attenuated (A)	6.4619	6.1075	5.7785
Low Pass Filtered (LP)	8.4233	7.9565	7.5237

MTFA-PERFORMANCE CORRELATIONS

Table 11 contains the independent correlations of several expressions of MTFA and performance measures. Each correlation is based on nine pairs

of points consisting of the MTFA expression and mean performance measure associated with the three systems and the three noise levels used during the experiment.

Table 11. CORRELATIONS BETWEEN MTFA AND PERFORMANCE AND EYE MOVEMENT MEASURES

MTFA	$\bar{X} R(M)$	$\bar{X} R(Z)$	$\bar{X} F D$	$\bar{X} S D$	$\bar{X} R(C)$	N Cor.
Perpendicular (\perp)	0.730*	0.716*	-.461	0.372	0.244	0.593
Parallel (\parallel)	0.118	0.138	-.553	0.560	-.108	0.231
Arithmetic Mean ($\perp + \parallel$)/2	0.532	0.533	-.577	0.542	0.103	0.500
Quadratic Mean [(\perp) ² + (\parallel) ²] ^{1/2}	0.392	0.400	-.592	0.587	0.028	0.414
Geometric Mean ($\perp \cdot \parallel$) ^{1/2}	0.642	0.636	-.535	0.474	0.171	0.559
Harmonic Mean 2/(\perp) ⁻¹ + (\parallel) ⁻¹	0.696*	0.686*	-.498	0.422	0.210	0.583

* $p < 0.05$.

NOTES: $\bar{X} R(M)$, mean ground range with minimum range substituted on incorrect trials; $\bar{X} R(Z)$, mean ground range with zero substituted on incorrect trials; $\bar{X} F D$, mean fixation duration; $\bar{X} S D$, mean saccade duration; $\bar{X} R(C)$, mean ground range calculated excluding incorrect trials; N Cor., number of correct responses.

As can be seen from table 11, the correlations between MTFA expressions and performance measures were generally low. This may be due, in part, to the low number of data points associated with each correlation. Two significant correlations were obtained ($ps < 0.05$): between perpendicular MTFA and (1) mean ground range with minimum range substituted on incorrect trials, and (2) mean ground range with zero substituted on incorrect

trials. These results are consistent with the analyses of variance cited previously which showed that the low-pass system yielded the smallest ground ranges. These same two ground range measures were significantly ($p < 0.05$) correlated with the harmonic mean of the perpendicular and parallel MTFAs.

Although not statistically significant ($p > 0.05$), the MTFA-eye movement correlations show a consistent trend. As MTFA decreases, mean fixation duration increases and mean saccade duration decreases.

IV. METHOD: STATIC IMAGERY EXPERIMENT

EXPERIMENTAL DESIGN

The experimental design was a full factorial 4 × 3 (Systems × Noise Level) experiment. Systems was a between-subjects variable and Noise Level was a within-subjects variable. The experimental design is illustrated in figure 13, which shows that each subject was presented with either an open system, an attenuated system, a low-pass filtered system, of a high-pass filtered system. Each of three noise levels, 0 mV rms, 55 mV rms, or 110 mV rms, was presented to each subject.

RMS NOISE	110V	S ₁ ⋮ S ₅	S ₆ ⋮ S ₁₀	S ₁₁ ⋮ ⋮	
	55V	S ₁ ⋮ S ₅	S ₆ ⋮ S ₁₀		
	0V	S ₁ ⋮ S ₅	S ₆ ⋮ ⋮		⋮ ⋮ S ₂₀
		OPEN	LOW PASS	HIGH PASS	ATTEN- UATED
		SYSTEM			

Figure 13. Static Imagery Experimental Design.

APPARATUS

Variable Parameter Television System

The television system used during the course of this experiment was essentially the same as that described for the previous experiment. The line rate for the system was 945 lines per frame and the frame rate was 30 frames per second, with a 2:1 positive interlace. As in the previous experiment, the observer's monitor was a Conrac Model QQA-17 equipped with a P-4 phosphor. The configuration of the system is presented in figure 14. The TV camera and monitor were oriented so that the raster was horizontal and the displayed picture had a 4:3 (horizontal:vertical) aspect ratio.

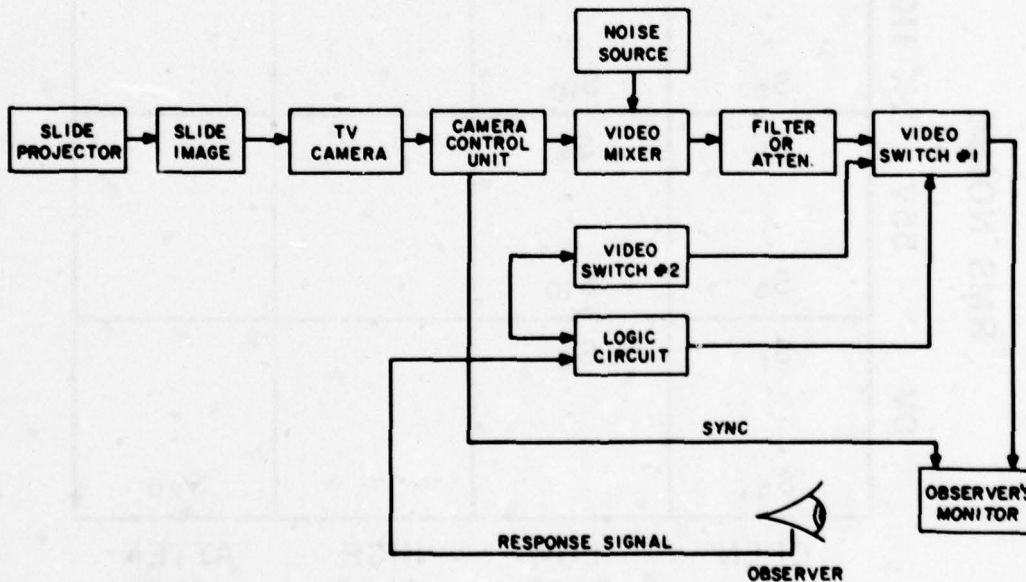


Figure 14. Simplified Block Diagram of Static Imagery Video System.

Image Quality Manipulation

Four different image quality conditions were produced by either passing, high-pass filtering, low-pass filtering, or attenuating the output of the camera control unit. The high-pass filter 3-dB point occurred at 5 MHz and the 3-dB downpoint of the low-pass filter occurred at 1.3 MHz. Seven dB of attenuation was achieved by passing the video signal through a Tektronix 2701 step attenuator.

Additionally, image quality was varied by combining 0, 55, or 110 mV rms of white electrical noise with the video signal. The output of a General Radio Model 1383 Random Noise Generator, which provided white noise over a range from 20 Hz to 20 MHz, was combined with the camera control video signal in a custom-designed wideband video mixer. Noise measurements were made before attenuation or filtering, using a Ballantine Model 323-01 True RMS voltmeter.

In order to insure uniform monitor black reference level setting, a noise-free video signal was provided during that portion of the video signal used for black level setting. Through the use of a specially designed video switch (Video Switch 1 in figure 14), a noise-free video signal was provided during vertical and horizontal retrace. The addition of a second video switch permitted blanking of the observer's monitor after target acquisition.

Stimuli

The stimuli viewed by the subject consisted of slides containing 34 randomly positioned letters and numerals. The letters and numerals were all of the Leroy font, were all of the same font size, and subtended

8 min of arc vertically and 5 min of arc horizontally. Each slide contained the letters A through Z and the numerals 2 through 9 without repetition of any character.

Stimulus Generation

A Kodak Model 800 Carousel slide projector was used to project the image of each target's slide onto a small screen which, in turn, was imaged by the video system camera. The slides were advanced under computer control, as indicated in figure 15. Synchronization for the video system camera was obtained directly from the camera control unit.

Behavioral Data Acquisition System

During the course of a subject's search for a target, the subject's eye rotations were tracked by an SRI International Dual Purkinje Image tracker. Eye position X and Y coordinates, valid position, and keypad response channels, as shown in figure 15, were sampled once every 2 ms by a PDP 11/10 computer. The sampled information was continuously written out to magnetic tape.

The subject used an 8-button keypad, located on the right arm of the subject's chair, to indicate target acquisition, location of the target, and readiness for the next slide. The subject's button press indicating target acquisition stopped eye movement data collection and blanked the monitor. The subject indicated the location of the target by pressing one of six buttons corresponding to areas formed by dividing the screen in half along the horizontal axis and into thirds along the vertical axis of the monitor. The subject's button press indicating the target location resulted in a corresponding voltage which was written out to

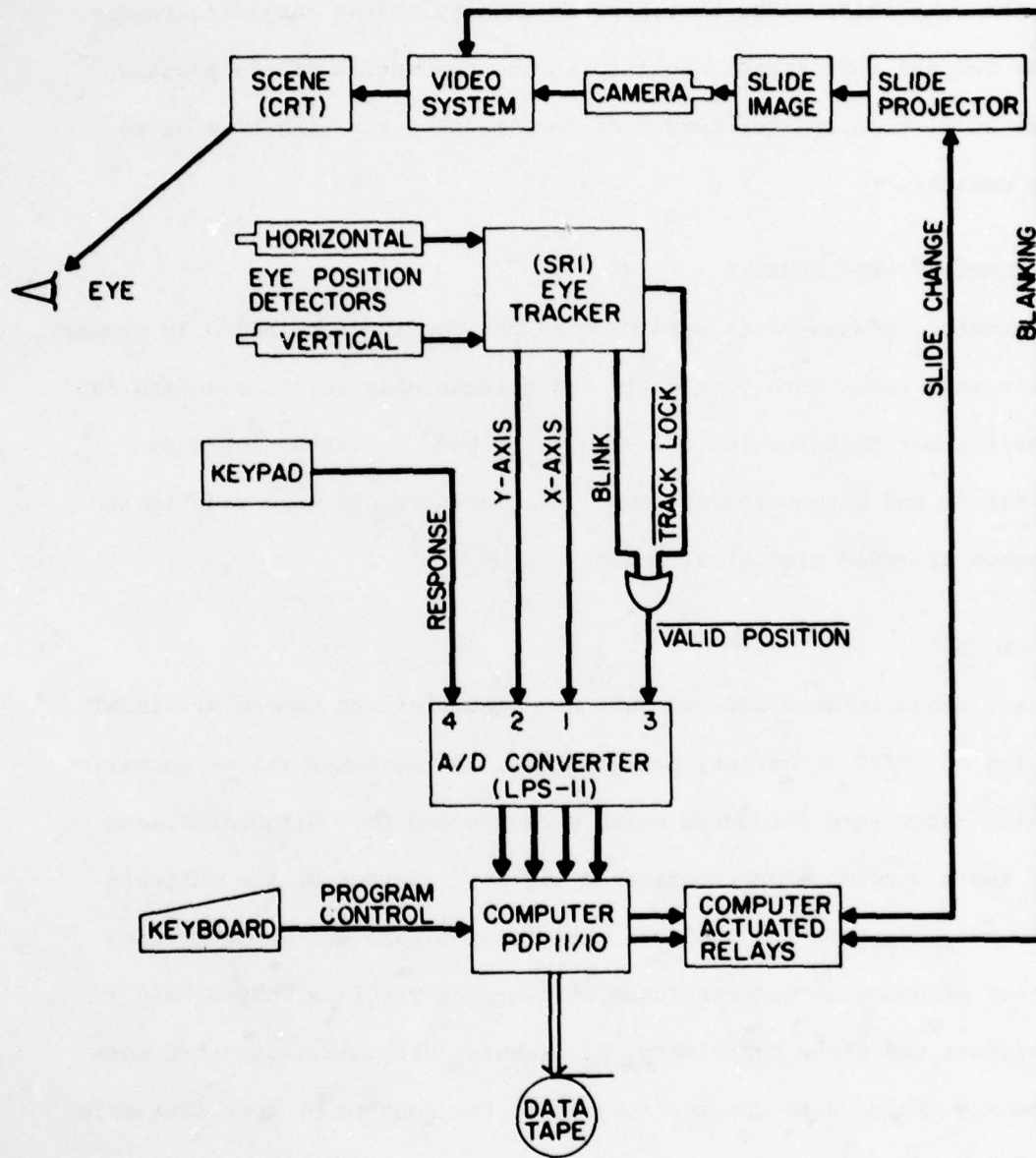


Figure 15. Simplified Block Diagram of Static Imagery Eye Movement and Behavioral Data Acquisition System.

magnetic tape as well as a signal which was used to close a second computer-controlled relay which caused the slide projector to advance to the next slide. The button press signifying the subject's readiness for the next target resulted in the resumption of eye position data collection and the return of the image of the target slide to the monitor.

PHOTOMETRIC MEASUREMENTS

Photometric measurements were made as previously described. In summary, scans were taken both vertically and horizontally across standard 1951 USAF tri-bar patterns for the open, high-pass filtered, low-pass filtered, and attenuated systems. All measurements were made in the absence of added electrical noise.

SUBJECTS

Twenty subjects were selected who had binocular and monocular visual acuity of 20/20 or better, near and far, and no other visual anomalies. Vision tests were conducted using a Bausch and Lomb Orthorater, and all tests were made on uncorrected vision. Sixteen of the subjects were male, four of the subjects were females, and all subjects were either graduate or undergraduate students at Virginia Polytechnic Institute and State University, Blacksburg, Virginia. Subjects were randomly assigned to groups, subject to the constraint that four male subjects and one female subject be assigned to each between-subjects group. All subjects were volunteers and were paid \$2.50 per hour for their participation.

PROCEDURE

Each subject participated in a preexperimental session similar to the one previously described. In summary, the preexperimental session consisted of informing the subject as to the purpose of the experiment, making a bite bar for the subject, establishing a bite bar position in which track lock could be established, and insuring that the tracker could maintain track lock over the entire monitor. In order to assess the stability of track lock, the subject was directed to fixate on each of 25 crosses arranged in a 5×5 array. The image of the crosses was generated by projecting a slide of the matrix onto the screen imaged by the video system camera. In those instances where track lock could not be reliably maintained as the subject fixated each of the crosses, the subject was paid for his/her time and dismissed.

Each experimental session was preceded by a calibration of the video system. The calibration was performed by placing a slide of a gray scale into the slide projector used for the target slides. Video signal amplitude was adjusted to a predetermined value by adjusting the gain and blanking level of the camera control unit. Signal amplitudes were monitored with an oscilloscope which was synchronized to the line rate of the video system. Once the signal levels being sent to the observer's monitor were set, the monitor's brightness and contrast controls were adjusted to yield a gray scale with predetermined luminances. These luminances were monitored using a Minolta "Autospot II" light meter.

Upon arrival, each subject was read a description of the experiment and was informed that the purpose of the study was to examine the

effects of image quality on eye movements, and that the task to be performed consisted of pressing a button as soon as he/she found a target letter or numeral which was located among randomly positioned letters and numerals. Subjects were instructed to locate a target for each trial and, if they could not locate the assigned target, they were to locate a target most similar to it. Each subject was told that this first button press would result in the screen being blanked and that the subject was to indicate the sixth of the screen in which the target letter or numeral was located by pressing one of six corresponding buttons. The subject's instructions indicated that after the location had been identified and after the next target letter or numeral had been given, the subject was to press another button indicating that he/she was ready for the next trial.

Each subject was given 117 trials, the first 15 of which were practice trials. Five practice trials were given at each of the three noise levels presented to each subject. The remaining 102 trials were divided into 6 series of 17 trials each. During each series, either 0, 55, or 110 mV of electrical noise was added to the video signal. Each subject received a randomly chosen order of noise levels, subject to the constraints that no two sequential series have the same noise level, no noise level appeared more than twice over the six series presented to each subject, and that the probability of a noise level being assigned to a series was approximately equal for any given subject.

During the course of each series, the subject was instructed to locate each of 17 letters and numerals, and over the course of two

noncontiguous series attempted to locate each of the letters A through Z and the numerals 2 through 9. Thus, each subject had to locate each of 34 characters under each of the three noise conditions. The sequence of targets to be located was randomly chosen, subject to the constraint that no target letter or numeral was repeated within the same noise level. The stimulus slides were made up of duplicates of 20 original slides. The sequence of slides was randomly chosen, subject to the constraints that no more than two duplicates of an original could occur within a series and that no two sequential slides were identical. All subjects received the same order of slides and targets. The end of each series was followed by a three minute rest period. The room illuminance was kept at 20 lux throughout the course of the experiment, and the observer's monitor was placed 101.6 cm away from the subjects.

V. RESULTS: STATIC IMAGERY EXPERIMENT

TARGET ACQUISITION PERFORMANCE ANALYSIS

The correctness or incorrectness of each subject's response to each target was determined by comparing the target location indicated by the subject with the known location of the target. The subject indicated apparent target location by pressing one of six buttons located on a keypad affixed to the arm of the subject's chair. If a target were located at or near the intersection of two adjacent areas, a response to either area was counted as correct.

The mean number of correct responses was calculated for each subject across the trials associated with each noise level. The results of a 4×3 analysis of variance (System \times Noise Level) performed on mean number of correct responses are presented in table 12, from which it may be seen that there were no significant main effects nor was the interaction significant ($ps > 0.10$).

Search times were measured from the time the image of the target slide was presented to the subject to the time the subject pressed a button indicating target acquisition. Mean search times were calculated for each subject across the trials associated with each noise level.

Table 13 presents the results of an analysis of variance performed on mean search times. The main effects of System and Noise Level and the System \times Noise Level interaction were all significant ($p < 0.001$).

From figure 16, which shows mean search time as a function of System

Table 12. SUMMARY OF ANALYSIS OF VARIANCE PERFORMED ON MEAN NUMBER OF CORRECT RESPONSES

Source of Variance	SS	df	MS	F	p
Systems (Sys)	1375.27	3	458.52	0.54	> 0.10
Subjects within Systems (S/Sys)	13589.44	16	849.34	----	----
Noise Level (NL)	711.93	2	355.97	2.26	> 0.10
Sys × NL	785.16	6	130.86	0.83	> 0.10
NL × S/Sys	5036.90	32	157.40	----	----

Table 13. SUMMARY OF ANALYSIS OF VARIANCE PERFORMED ON MEAN SEARCH TIME

Source of Variance	SS	df	MS	F	p
Systems (Sys)	18072.16	3	6024.05	11.37	< 0.001
Subjects within Systems (S/Sys)	8476.98	16	529.81	----	----
Noise Level (NL)	3951.07	2	1975.54	10.91	< 0.001
Sys × NL	8266.95	6	1377.83	7.61	< 0.001
NL × S/Sys	5793.22	32	181.04	----	----

and Noise Level, it can be seen that the source of the interaction is the long mean search time associated with the high-pass filtered system at the 110 mV noise level. Newman-Keuls tests revealed that the high-pass filtered system with 110 mV of added noise yielded a mean search time which was significantly greater than all other mean search times

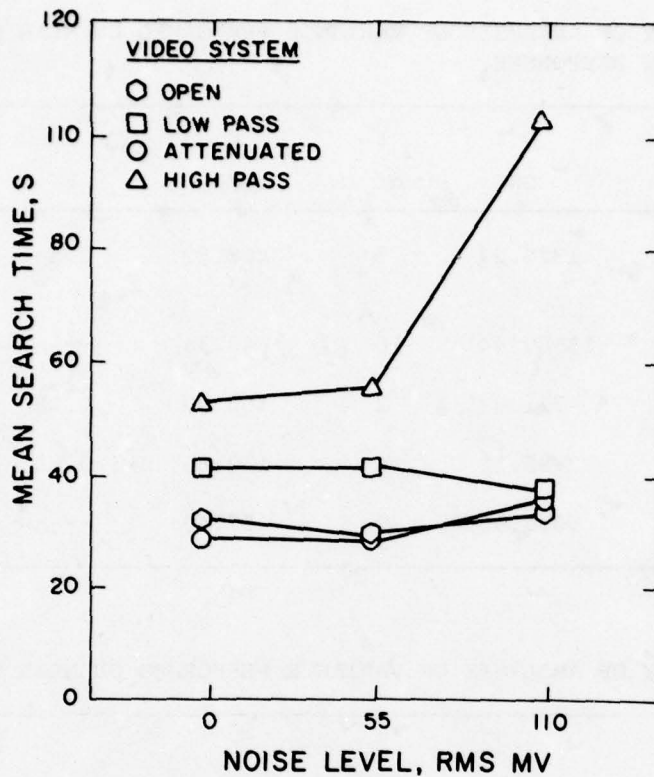


Figure 16. Static Imagery Experiment: Mean Search Time as a Function of Noise Level and System

($p < 0.01$). These tests also revealed that none of the other mean search times differed from each other ($p > 0.01$).

EYE MOVEMENT DATA REDUCTION

Eye movement data reduction consisted of classifying data points as indicating fixation or saccadic movement. The classification of the eye movement data was based on estimates of instantaneous velocity and acceleration, as described for the previous experiment. Mean fixation and saccade durations were calculated for each target. If, during the course of the subject's search, track lock was not established, mean durations of zero were reported.

EYE MOVEMENT PERFORMANCE

Table 14 contains the results of an analysis of variance performed on mean fixation durations. Mean durations were calculated by taking the mean of the non-zero fixation durations for each target within a noise level. The results of the analysis of variance indicate a significant effect of system ($p < 0.002$), a significant effect of Noise Level ($p < 0.001$), and a significant System \times Noise Level interaction ($p = 0.007$). Figure 17, which depicts mean fixation duration as a function of Noise Level and System, shows that the mean fixation durations for the high-pass system were 50% greater than those obtained from the other systems, and that this effect was most pronounced at the 110 mV noise level. Pairwise comparisons performed with Newman-Keuls tests indicated that the mean fixation durations of the attenuated, open, and low-pass systems did not differ among each other at any noise level ($p > 0.01$). These comparisons also revealed that mean fixation durations associated with the high-pass system at 0 mV and 55 mV rms did not differ from each other ($p > 0.01$), and that they did differ from all the mean fixation durations associated with open, low-pass, and attenuated systems ($p < 0.01$). The mean fixation durations obtained from the high-pass 110 mV rms noise level condition differed from all other means ($p < 0.01$).

The results of an analysis of variance performed on mean saccade durations are contained in table 15. As can be seen, none of the main effects or interactions were statistically significant ($p > 0.10$).

Table 14. SUMMARY OF ANALYSIS OF VARIANCE PERFORMED ON MEAN FIXATION DURATION

Source of Variance	SS	df	MS	F	p
System (Sys)	295341.75	2	98447.25	6.23	< 0.002
Subjects within Systems (S/Sys)	252952.63	16	15809.54	----	----
Noise Level (NL)	41054.31	2	20527.16	20.40	< 0.001
Sys × NL	22064.64	6	3677.44	3.65	0.007
NL × S/Sys	32200.84	32	1006.28	----	----

Table 15. SUMMARY OF ANALYSIS OF VARIANCE PERFORMED ON MEAN SACCADE DURATION

Source of Variance	SS	df	MS	F	p
System (Sys)	347.32	3	115.77	0.30	> 0.10
Subjects within Systems (S/Sys)	6115.94	16	382.25	----	----
Noise Level (NL)	197.46	2	98.73	2.06	> 0.10
Sys × NL	330.75	6	55.13	1.15	> 0.10
NL × S/Sys	1530.91	32	47.84	----	----

PHOTOMETRIC DATA REDUCTION

As in the previous experiment, the photometric scans of displayed tri-bar patterns were analyzed using numerical Fourier analysis. In order to meet the assumption that the data analyzed must contain an integral number of cycles, each scan was trimmed to yield a maximum modulation at the spatial frequency of the fundamental. The fundamental spatial

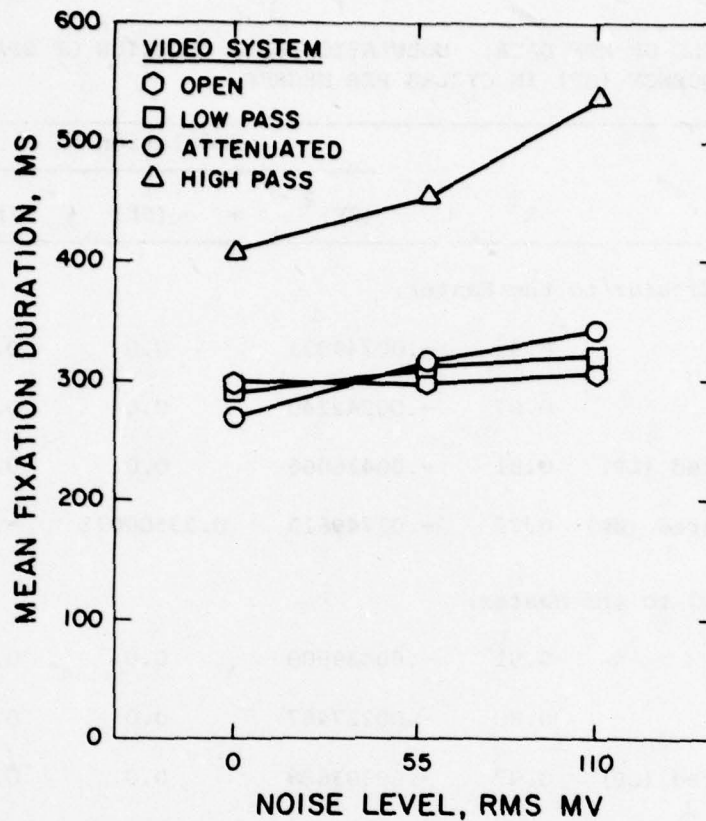


Figure 17. Static Imagery Experiment: Mean Fixation Duration as a Function of Noise Level and System

frequency and the associated modulation were thus obtained for each scan, and are contained in Appendix C.

MTFA-PERFORMANCE CORRELATIONS

An expression for each system's MTF curve was obtained by fitting quadratic models to the spatial frequency-modulation data obtained for each system. The coefficients of each model were obtained using a multiple regression fit, the results of which are contained in table 16.

MTFAs were obtained by solving

$$MTFA = \int_{i1}^{i2} [F_1(SF) - F_2(SF)] d(SF) \quad (2)$$

Table 16. MODELS OF MTF DATA: MODULATION AS A FUNCTION OF SPATIAL FREQUENCY (SF) IN CYCLES PER DEGREE

System	R ²	Modulation =		
		(SF) ²	+ (SF) +	Intercept
<i>Targets Perpendicular to the Raster:</i>				
Open (O)	0.83	-.00349031	0.0	0.65917760
Attenuated (A)	0.67	-.00242240	0.0	0.38886775
Low-Pass Filtered (LP)	0.81	-.00426066	0.0	0.25291780
High-Pass Filtered (HP)	0.77	-.01749615	0.23500071	-.36314513
<i>Targets Parallel to the Raster:</i>				
Open (O)	0.91	-.00439900	0.0	0.73836799
Attenuated (A)	0.80	-.00227467	0.0	0.43420765
Low-Pass Filtered (LP)	0.97	-.00383688	0.0	0.68075501
High-Pass Filtered (HP)	0.22	-.00010104	0.0	0.03551667

where

$F_1(SF) =$ MTF equation,

$F_2(SF) =$ threshold equation,

SF = spatial frequency,

$i_1 = 0$ except for the high-pass filter condition where $i_1 =$ the intersection of the MTF and threshold curves, and

$i_2 =$ intersection of the MTF and threshold curves.

MTFA values are contained in table 17. The expression used for the threshold detectable modulation curves was the same as that used in the previous experiment, as the line rate and noise conditions were identical.

Table 17. CALCULATED MTFAS FOR EACH COMBINATION OF SYSTEM AND NOISE LEVEL

System	Noise Level		
	0 mV	55 mV	110 mV
<i>Targets Perpendicular to the Raster:</i>			
Open (O)	5.9131	5.5920	5.2942
Attenuated (A)	3.1725	2.9084	2.6737
Low-Pass Filtered (LP)	2.2512	1.9427	1.6902
High-Pass Filtered (HP)	2.7746	2.5415	2.3187
<i>Targets Farallel to the Raster:</i>			
Open (O)	6.2551	5.9678	5.6979
Attenuated (A)	3.8703	3.5546	3.2726
Low-Pass Filtered (LP)	5.9200	5.6178	5.3360
High-Pass Filtered (HP)	0.2786	0.0684	0.0291

Table 18 contains the independent correlations between several expressions of MTFA and performance measures. Each correlation is based on 12 pairs of points consisting of the MTFA expression and the mean performance measure associated with the four Systems and three Noise Levels.

Of considerable interest, in table 18, are the significant correlations between MTFA and mean search time ($ps < 0.05$) and mean fixation duration ($ps < 0.005$). The correlations with mean search time indicate that as MTFA increases, the search time decreases. The importance of the parallel MTFA component is indicated by the fact that the MTFA parallel-mean search time correlation is significant, while the MTFA perpendicular-mean search time correlation is not. This result is consistent with the

Table 18. CORRELATIONS BETWEEN MTFA AND PERFORMANCE AND EYE MOVEMENT MEASURES

MTFA	\bar{X} N Cor.	\bar{X} ST	\bar{X} FD	\bar{X} SD
Perpendicular (⊥)	-.349	-.367	-.364	0.212
Parallel ()	0.332	-.684*	-.864**	-.311
Arithmetic Mean (⊥ +)/2	0.088	-.661*	-.791**	-.133
Quadratic Mean [(⊥) + ()] ^{1/2}	0.109	-.632*	-.774**	-.128
Geometric Mean (⊥ ·) ^{1/2}	0.104	-.703*	-.823**	-.149
Harmonic Mean 2/(⊥) ⁻¹ + () ⁻¹	0.064	-.695*	-.807**	-.174

*p < 0.05. **p < 0.005.

NOTES: \bar{X} N Cor., mean number correct; \bar{X} ST, mean search time; \bar{X} FD, mean fixation duration; \bar{X} SD, mean saccade duration.

observations that the high-pass filtered system and high noise level condition was the only condition which significantly lengthened search times and that the high-pass filtered system produced the greatest MTFA difference for targets oriented parallel to the raster.

The effect of the high-pass filter on the system MTF, and hence the parallel MTFA, is due to the orientation of the major axis of the tri-bar pattern and nature of the high-pass filter. Each bar of the tri-bar pattern is five times as long as it is high. As illustrated in figure 18, when the tri-bar pattern was oriented parallel to the raster, this means that the major axis of each bar was parallel to the raster structure. The direction of a photometric scan of the tri-bar pattern

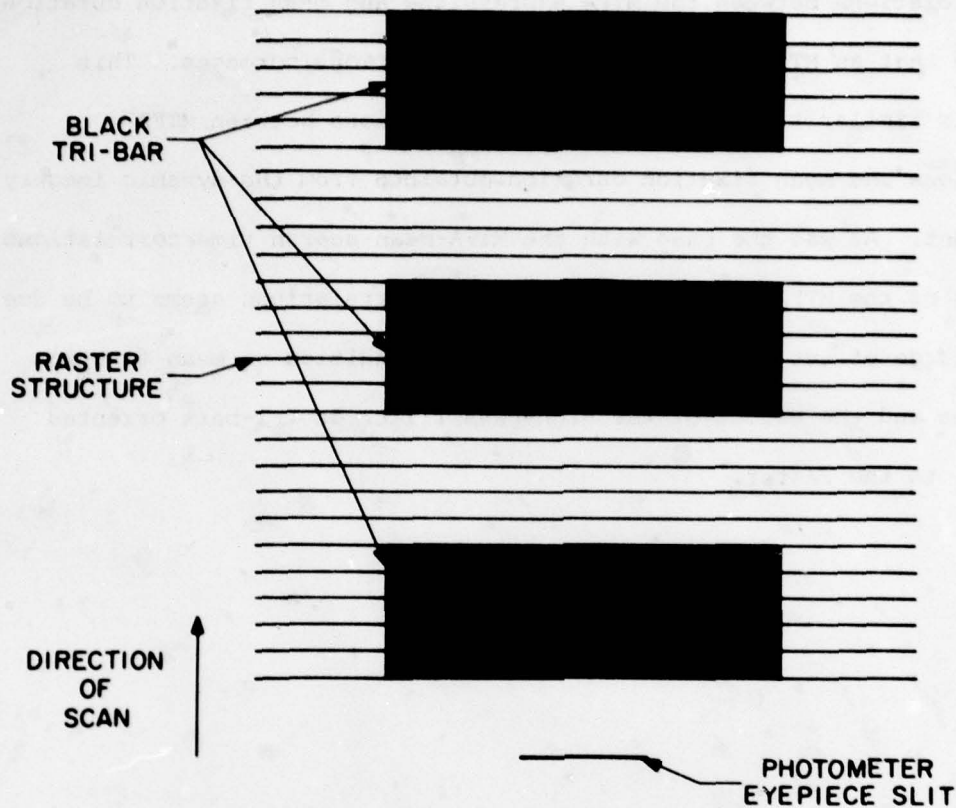


Figure 18. Diagram of Block Tri-Bar Showing Pattern Oriented Parallel to Raster Structure, Eyepiece Slit, and Direction of Scan.

was perpendicular to the raster with the major axis of the eyepiece slit oriented parallel to the raster structure.

Since the high-pass filter removes the DC and low-frequency components along the major axis of each bar of the pattern oriented parallel to the raster only the leading and trailing edges of the pattern remain. As the slit is moved across the tri-bar pattern, there is little change in the recorded luminance level, since the center portion of the tri-bar pattern has been removed. Hence, the modulation and MTF calculated from such a scan will approach zero.

The correlations between the MTFA expressions and mean fixation duration indicate that as MTFA decreases, fixation duration increases. This result is similar to the trend in the correlations between MTFA expressions and mean fixation duration obtained from the dynamic imagery experiment. As was the case with the MTFA-mean search time correlations, the form of the MTFA-mean fixation duration correlations seems to be due to the large effect of the high-pass filter condition on mean fixation durations and the effect of the high-pass filter on tri-bars oriented parallel to the raster.

VI. DISCUSSION AND CONCLUSIONS

TARGET ACQUISITION PERFORMANCE

The effect of System and Noise Level on performance in both experiments was largely as expected. The System variable had no significant overall effect on the number of correct target acquisitions in either experiment; however, the high-pass filtered system produced longer search times in the static experiment, while the low-pass filtered system produced shorter acquisition ranges in the dynamic study. Of interest is the fact that the -7 dB attenuated system had no demonstrable effect upon any performance measure in either experiment.

The Noise Level variable did not affect the number of targets acquired in the static display experiment, but increases in noise led to decreases in the number of targets acquired in the dynamic experiment. In the static experiment, the 110 mV noise level led to longer search times for the high-pass system only, while Noise Level had no effect on range in the dynamic experiment.

Target size effects are largely as expected in the dynamic study. As target size increases, targets are acquired more frequently and at greater ranges.

MTFA UTILITY

In both experiments, correlations between MTFA values and target acquisition performance were fair to good, and in the expected directions. In the dynamic imagery experiment, the perpendicular

MTFA value correlated significantly with both weighted acquisition range measures ($r > 0.716$), as did the harmonic mean of the perpendicular and parallel MTFA values ($r > 0.686$). This result is most likely due to the large contribution of the perpendicular component. This is to be expected because the perpendicular MTFA is affected by video passband, whereas the parallel MTFA is largely unaffected (except in the case of a high-pass system, as indicated previously). The MTFA measures did not correlate significantly with the number of correct targets acquired or with eye movement measures, although some suggestion of a relationship with fixation duration is seen.

In a similar fashion, increases in MTFA values generally led to decreases in search time in the static display study. Except for the perpendicular MTFA measure, all correlations were significant ($r > 0.632$).

Thus, as found in previous experiments (e.g., Snyder, 1976; Snyder et al., 1974), there is a fair correlation between image quality as measured by the MTFA and operator performance, although this correlation is not as great as might be desired for careful system design tradeoffs. The remaining unpredicted variation in most experiments is substantial.

The correlations obtained in these experiments are certainly not as high as those found by Task (1979). A possible explanation lies in the fact that Task's manipulations of MTFA did not include variation in noise level, whereas the present studies did.

The MTFA is clearly anisotropic, as indicated by these results. First, the high-pass system was usable, albeit poor, for the static experiment, and totally unusable for the dynamic display task. The perpendicular

MTFA for the high-pass system is somewhat larger than that for the low-pass system in the static experiment, at all three noise levels, yet performance is better for the low-pass system. Of course, the parallel MTFA is much greater for the low-pass than for the high-pass system, and the parallel MTFA for the high-pass system is near zero. In part, the correlations between performance and MTFA may be due to inappropriate combination of these parallel and perpendicular MTFA values.

The second, and perhaps best, example of anisotropy can be seen with the consistent lack of difference in performance between the open and -7 dB attenuated systems. Comparing these two systems only, for both the static and dynamic studies, one finds that the MTFA values differ from 52% to 92%; yet, no significant difference in any performance measure was obtained in either experiment. That is, reduction in the MTFA by lowering substantially the image modulation across *all spatial frequencies* has no significant effect on target acquisition performance. Stated another way, the MTFA contribution near the detection threshold curve appears to be much more important than is the contribution of the area nearest to the MTF curve.

EYE MOVEMENT RESULTS

The saccade duration measure was consistently insensitive to image quality variation, whereas the fixation duration measure varied in an expected manner with System in the static display experiment. In this study, the high-pass system resulted in 50% longer fixation durations than did any other system, and this difference was more pronounced at the highest (110 mV) Noise Level.

While the System and Noise Level variables had no effect on eye movement measures in the dynamic experiment, it was noted that the mean fixation duration in the dynamic display experiment was 510.01 ms as compared to 347.16 ms in the static display experiment. This difference is surprisingly large, and it may be due to the greater display complexity or task difficulty in the dynamic experiment than in the static experiment. While previous researchers (e.g., Gould, 1969; Snyder and Taylor, 1976) have suggested that fixation durations increase with display complexity, none have suggested a difference of this magnitude. Further research along these lines is warranted and suggested.

Statistically speaking, the mean fixation duration measure was not as sensitive to System and Noise Level variation as were performance measures such as search time (static experiment) and number correct (dynamic experiment). Nonetheless, the correlation between fixation duration and MTFA were consistently negative ($-.592 < r < -.461$ for dynamic and $-.864 < r < -.364$ for static), with the only significant correlations involving the parallel MTFA measure in the static experiment. As MTFA increases, mean fixation duration consistently decreases. Fixation durations, as an index of image quality, should be researched further.

Lastly, it can be seen that mean fixation durations increase as either search time increases or, equivalently, range decreases (in the dynamic experiment). The correlation between fixation duration and search time is $r = 0.92$ in the static experiment; in the dynamic experiment, $r = 0.55$

between fixation duration and the two substituted range measures. Thus, results of these two experiments strongly suggest that search performance may well be predicted by fixation duration measures or, equivalently, that image quality may be sensitively measured by fixation durations. Further research on this topic is strongly suggested.

APPENDIX A: PROCEDURES USED TO ESTABLISH

TRACK LOCK

INTRODUCTION

The purpose of this appendix is to describe the operating procedures used in conjunction with an SRI dual Purkinje image eyetracker. It is assumed that the user is in possession of and familiar with a Dual Purkinje Image Eyetracker Manual published by SRI International. Several terms used throughout the description of the procedure are described below. The input optics refer to the collection of lenses and mirrors which define the optical path between the light source and the dichroic mirror. The receiving optics are the collection of lenses, mirrors, beamsplitters, and detectors which define the optical path between the dichroic mirror and the photodetectors for the first and fourth Purkinje images.

The input optics contain two sources of energy--the visible source and the infrared (IR) source. Throughout the procedure, if the IR source is to be used, it is assumed that the user has moved the IR/Visible source lever to the infrared position and has switched the electronics front panel selector switch to the IR position. Similarly, if the visible source is indicated as being operational, it is assumed that the source lever and selector switch have been moved to their appropriate positions.

The iris diaphragm refers to the iris located between the source and the mirrors driven by the first Purkinje image servo. This iris

diaphragm is used for varying the size of the source beam. The centering light is a source of visible illumination located below the dichroic mirror. If this source is mentioned as being operational, it is assumed that the user has energized the source by pressing the appropriate button on the front panel of the electronic package.

In the receiving optics, M13 refers to the adjustable mirror used to control the position of the fourth Purkinje image on the fourth Purkinje image photodetector. The fourth detector lever refers to that lever which allows the operator to slide the fourth Purkinje image detectors into the receiving optical path. The IR viewer refers to the infrared scope placed behind the fourth Purkinje image detectors.

The goal of this operating procedure is to establish stable tracking of eye rotations over as much of the subject's display as possible. The situation may be visualized as trying to superimpose the trackable field of view onto the observer's display. The trackable field of view refers to the angular area over which the eyetracker can maintain track lock. Stable tracking of eye rotations is referred to as track lock.

In the context of the present research, the trackable field of view was symmetrically superimposed about the center of the subject's monitor. As a result, track lock was maintained as the subject scanned across the entire display.

OPTICAL CONFIGURATION AND THE TRACKABLE FIELD OF VIEW

The SRI eyetracker is capable of being used in the wide-range, mid-range, and narrow-range optical configurations. As one moves from wide to narrow range, the trackable field of view decreases. The loss of

trackable field of view is offset by a decrease in the minimum pupil size for which track lock remains stable. Since, as the luminance of the display increases pupil size tends to decrease, as one moves from wide-range to narrow-range configurations the luminance of the display may be increased. The present studies were run using the narrow-range optical configuration. The maximum display luminance was 68 cd/m^2 .

BITE BAR FITTING

A bite bar used was constructed of 3.2 mm thick aluminum sheet metal. The "U" shaped part of the bite bar was 58 mm by 58 mm. Each arm of the U was 11 mm across. At the bottom portion of the U, a 24 mm stalk was cut. This stalk served as the attachment to a modified machinist's stage used in positioning the bite bar. The bite bar was covered with Kerr Manufacturing Company green stick compound. The bite bar was covered with approximately 14 mm of compound. All exposed metal, except for the stalk, was covered with the compound. An impression of the subject's teeth was made by heating the bite bar and having the subject bite down on the softened compound.

Once the dental impression had been made and the bite bar had cooled down, the bite bar was attached to a machinist's stage. This stage moved horizontally (X), vertically (Y), and axially (Z). The stage was modified to accept a bite bar holder and forehead rest. Alignment of the subject with the tracker was obtained by moving the subject in X, Y, and Z as indicated in the procedure outlined below.

INITIAL ALIGNMENT

The subject was placed in a chair equipped with a hydraulic lift. This enabled the experimenter to position the bite bar and then to move the

subject to the bite bar. As the procedure progressed, adjustments were made in the chair height in order to insure the subject's comfort.

The initial alignment of the subject to the tracker was achieved using visible light provided by the two sources. One source, the visible source, is located in the same plane as the infrared source and follows a path through the dovetail mirror assembly. This optical path leads the beam of light to the dichroic mirror and onto the subject's eye. The image from the visible source forms a red and white crescent of light on the subject's eye. These crescents of light are used to align the subject in the X-Y planes. The second source, the centering light, projects an elliptically shaped white spot of light onto the subject's eye. The centering light is used to align the subject in the Z plane.

The images from the visible source and the centering light come closest to intersecting at one point in the X, Y, and Z planes. This can be seen by placing a sheet of paper some 15 cm behind the dichroic mirror and moving a sheet of paper toward the dichroic mirror. The point at which the three images, two from the visible source and one from the centering light, come closest to intersecting is the desired location of the subject's eye.

The initial alignment is made with the subject looking straight ahead at the center of the display he/she will be viewing. The center of the display should intersect a ray extended from the intersection of a vertical plane located 4 cm from the left edge of the dichroic mirror and a horizontal plane located 9 cm from the eyetracker baseplate.

Step 1: Activate the visible source and the centering light. Open the iris diaphragm to its maximum aperture.

Step 2: Move the bite bar in X, Y, and Z until the subject's right eye is 5 cm behind the dichroic mirror, 3 cm from the left edge of the dichroic mirror, and 1 cm from the top of the dichroic mirror.

Step 3: Move the subject and the bite bar in the X, Y, and Z planes until the images of the centering light and the two crescents from the visible source are near or on the subject's pupil.

Step 4: Adjust the subject in all three planes such that the image from the centering light falls within the pupil and the white crescent from the visible source outlines the edge of the subject's pupil. The red crescent should fall inside the pupil. This completes the initial alignment.

It is important to note that even if the subject is properly aligned at this stage, small changes in X, Y, and Z will be necessary as the procedure is continued. As the initial alignment comes close to criteria indicated above, only small changes in X, Y, and Z will be required. Due to the centering light's angle of incidence, changes in the X, Y, and Z position of the subject are needed to place the elliptical spot of light within the pupil boundaries.

OPTICAL ALIGNMENT

The purpose of the optical alignment procedure is to refine the alignment made during the initial alignment. This procedure involves trimming the IR source beam and positioning the subject with respect to the IR beam.

Step 1: Turn off the visible source and the centering light. Move the fourth detector lever so that the fourth Purkinje image photodetectors are out of the receiving optical path.

Step 2: Zero the servomechanisms by turning the H1, V1, H4, V4, and focus servo switches to the up position. This step should be taken with the IR source off and the search selector in the off position. After five seconds, turn all the servo switches off.

Step 3: Move the subject and the bite bar in the Z axis in order to focus the Purkinje images. The images are in focus when, looking through the IR viewer, the pupil boundary is sharpest and the brighter of the two spots within the pupil (the first Purkinje image) is sharpest, brightest, and best defined.

Step 4: With the subject looking at the center of the display, move the subject and the bite bar in the X and Y planes until the IR beam is concentric with the subject's pupil. This adjustment is made using the IR viewer.

Step 5: With the subject looking at the center of his/her display, reduce the size of the iris diaphragm until the beam of IR energy is coincident with and does not exceed the boundaries of the subject's pupil. This adjustment is made while the experimenter is looking in the IR viewer. If the smallest aperture setting yields a beam larger than the subject's pupil, give the subject a rest break and go to step 3. If during the next setting the smallest iris diaphragm setting yields a beam larger than the pupil, dismiss the subject. If the pupil is too small, the tracker will not be able to maintain track lock.

ALIGNMENT FOR CAPTURE

This portion of the procedure entails making adjustments in the location of the bite bar and the subject in order to facilitate the acquisition of track lock. In addition, further adjustments are made in superimposing the trackable field of view onto the display. In order to complete this part of the procedure, the experimenter will have to be able to discriminate between the first and fourth Purkinje images as they appear in the IR viewer. The first Purkinje image appears as a bright dot on the right side of the image of the pupil and the fourth Purkinje image appears as a very much dimmer and smaller dot to the left of the first Purkinje image.

This portion of the procedure begins where the previous section left off, namely, the IR source is on, the visible source and centering light are off, the image of the IR beam completely fills but does not exceed the boundaries of the pupil, and the search selector knob is in the off position.

Step 1: Turn the light level potentiometer to a setting of 7.4.

Step 2: While observing the first Purkinje image return meter, make small adjustments in the X, Y, and Z planes in order to maximize the first Purkinje image return signal, and in order to make the focus light come on. Focus adjustments are made in the Z plane. It is important to note that at this stage only small changes in X, Y, and Z are required. If the experimenter feels that he/she has moved the subject too far, then the experimenter may verify this by looking in the IR viewer. If the IR beam and the pupil are not coincident, then

the experimenter has moved the subject too far and the procedure should be repeated from the section and step where the beam and pupil are made coincident. If the subject is moved too far out of position, the iris will come into view and will reflect infrared energy. The reflection from the iris may cause an abnormally high first Purkinje image return signal. The experimenter should be careful not to try to establish track lock in this condition.

Step 3: Once the first Purkinje image return signal has been maximized and the focus servo light is intermittently or steadily lit, small changes in X, Y, and Z are necessary in order to zero the horizontal and vertical error meters for the first Purkinje image system. Adjust the light level potentiometer until the first return signal meter needle is located between 0.4 and 0.6. When the track lock lights are lit, the servos may be engaged and capture should be achieved. At this point, the focus servo may be energized. Turn the search selector knob to the auto position. The stability of track lock may be assessed by having the subject look around the display in a circle subtending no more than a few degrees.

Step 4: With the subject looking at the center of his/her display, the experimenter should check the relative position of the first and fourth Purkinje images. Looking through the IR viewer, the first and fourth images should appear to be on the same horizontal plane. If they are not, this may be changed by changing the height of the subject's display. The fourth Purkinje image should appear halfway between the outer edge of the pupil and the first Purkinje image. The horizontal position of

the fourth Purkinje image may be changed by moving the subject's display in its horizontal position.

Step 5: The establishment of fourth Purkinje image track lock is achieved by adjusting the thumb screws on M13 such that the image of the fourth appears under the cross hairs in the field of the IR viewer. Note these cross hairs are not necessarily located in the center of the viewer field of view. Slide the fourth photodetectors into the optical path. If the setting of the cross hairs is correct, the fourth track lock lights should be lit. The signal strength returned should cause a needle deflection to be within the boundaries marked on the fourth return meter. If the signal is not within bounds, the gain pot should be adjusted until the signal is within the bounds. Engage the H4 and V4 servomechanisms by moving the associated front panel switches to the up position.

STABILITY CHECK

The stability check is made on a calibration matrix consisting of at least a 3×3 array of lights, crosses, or small point sources. This array should cover the whole display field of view of interest. The purpose of this procedure is to make further adjustments in the X,Y position of the display in order to fully superimpose the trackable field of view onto the display field of view.

Step 1: Have the subject separately fix each of the points in the calibration matrix. This procedure should be started from the center of the display and should proceed to the corners of the matrix.

Step 2: Determine any corners over the calibration matrix where track lock is lost. If the track lock is lost in a particular corner, move the display toward the corner where track lock was lost. This may require moving the display in both X and Y planes. Repeat the procedure of having the subject separately fixate the calibration matrix. It is important to note that only small changes in the X,Y location of the display should be necessary. These changes should be no more than 3 or 4 cms in the X or Y directions. If the track lock is not stable, the experimenter has two options. The experimenter may dismiss the subject or may begin the procedure from the initial alignment procedure.

If track lock is unusually unstable, the experimenter should proceed to the optical alignment procedure. If pupil size has become too small, it may be necessary to give the subject a rest break or dismiss the subject.

APPENDIX B: DYNAMIC IMAGING SYSTEM MTF DATA

System	Tri-Bar Orientation	Spatial Frequency (cycles per degree)	MTF
Open	Perpendicular	2.5897	0.86511
		2.8836	0.77798
		2.9164	0.80012
		3.0033	0.81597
		3.1623	0.84878
		3.3648	0.72989
		5.1126	0.56443
		5.7482	0.51984
		6.1617	0.56537
		6.5034	0.48603
		6.6066	0.38699
Open	Parallel	8.6414	0.56481
		11.7992	0.19404
		2.0501	0.93404
		2.9164	0.79616
		3.1754	0.79599
		3.4830	0.81138
		4.1001	0.80786
		5.1815	0.80271
		5.3905	0.78115
		6.2476	0.65217
		6.2573	0.75040
6.8269	0.73099		
9.9418	0.61242		
9.1697	0.54669		
10.5885	0.50346		
12.6995	0.48781		
14.5729	0.25258		

System	Tri-Bar Orientation	Spatial Frequency (cycles per degree)	MTF
Low-Pass Filtered	Perpendicular	3.5616	0.25780
		3.5637	0.51819
		4.4770	0.25992
		5.1794	0.16857
		6.6460	0.15611
		6.8261	0.12896
		12.3004	0.02925
Low-Pass Filtered	Parallel	2.4740	0.79432
		3.1238	0.72917
		3.0269	0.78649
		4.5000	0.85253
		4.5373	0.62493
		4.5507	0.68655
		5.4285	0.66385
		6.1853	0.69958
		6.6338	0.71262
		6.7094	0.56393
		7.2735	0.62369
		8.0951	0.50395
		10.8650	0.44731
12.6995	0.37176		
13.6478	0.23870		

System	Tri-Bar Orientation	Spatial Frequency (cycles per degree)	MTF
Attenuated	Perpendicular	2.6603	0.55899
		2.9485	0.51791
		2.9571	0.49582
		3.1238	0.49386
		4.4215	0.39502
		5.3159	0.41170
		5.8746	0.38502
		6.5615	0.34190
		9.3373	0.22913
		9.6032	0.20038
		10.3216	0.15831
		11.5097	0.12682
12.0980	0.05660		
Attenuated	Parallel	2.8331	0.55918
		2.8944	0.77818
		3.0033	0.85993
		3.3087	0.85208
		4.1001	0.56152
		5.1641	0.52869
		5.5461	0.46685
		6.2003	0.42675
		6.9445	0.53013
		6.9495	0.39062
		7.4413	0.49450
		9.0253	0.39975
10.8696	0.33913		
12.2357	0.26593		

APPENDIX C: STATIC IMAGING SYSTEM MTF DATA

System	Tri-Bar Orientation	Spatial Frequency (cycles per degree)	MTF
Open	Perpendicular	2.7336	0.76016
		3.2019	0.76358
		4.2784	0.65198
		5.1794	0.58354
		5.7888	0.53866
		6.1262	0.45278
		6.3508	0.49649
		6.6900	0.42445
		7.5106	0.34417
		9.2221	0.22832
		10.2560	0.18484
		11.9744	0.17182
		12.1435	0.16408
12.2357	0.19161		
13.4627	0.13570		
Open	Parallel	2.4602	0.79586
		3.1754	0.77574
		3.1754	0.70586
		3.5310	0.62865
		4.5123	0.63161
		5.0809	0.60470
		5.6247	0.54996
		6.0976	0.58628
		6.1646	0.53928
		7.4413	0.48976
7.9065	0.40928		
9.6032	0.31483		
11.2604	0.24172		

System	Tri-Bar Orientation	Spatial Frequency (cycles per degree)	MTF
Low-Pass Filtered	Perpendicular	3.4988	0.29868
		4.5778	0.20248
		6.2573	0.18089
		6.3047	0.15978
		8.8322	0.16007
		10.9125	0.13608
		10.8285	0.11186
		12.9016	0.02606
Low-Pass Filtered	Parallel	3.1754	0.62390
		3.2019	0.67697
		3.8420	0.64183
		4.1084	0.59728
		6.6860	0.50828
		5.7698	0.53432
		6.2476	0.52023
		7.3064	0.51209
		7.6487	0.45121
		8.6414	0.35939
10.8285	0.27349		
11.1226	0.18126		

System	Tri-Bar Orientation	Spatial Frequency (cycles per degree)	MTF
High-Pass Filtered	Perpendicular	3.2288	0.21244
		4.3289	0.27453
		4.3373	0.31134
		5.1468	0.41724
		5.4094	0.43844
		6.1019	0.47324
		6.3497	0.39001
		7.3397	0.52464
		9.4901	0.20335
		10.0718	0.14971
	11.5097	0.12186	
High-Pass Filtered	Parallel	3.5782	0.04361
		4.4729	0.01864
		4.5643	0.02868
		8.9459	0.03962
		9.8407	0.03207
		12.5600	0.01125

System	Tri-Bar Orientation	Spatial Frequency (cycles per degree)	MTF
Attenuated	Perpendicular	3.4210	0.46511
		3.7690	0.44482
		4.1001	0.39986
		5.1126	0.32807
		5.6661	0.34326
		6.2476	0.27428
		6.2331	0.17056
		6.5297	0.23792
		7.4413	0.12778
		8.6880	0.13740
		11.7992	0.08617
12.1493	0.10287		
Attenuated	Parallel	2.8836	0.47467
		3.4988	0.45817
		4.0151	0.40238
		4.2548	0.37480
		4.5507	0.36452
		5.5436	0.34166
		6.7097	0.30582
		6.9408	0.34877
		7.6126	0.24674
		8.6953	0.21360
11.5924	0.18208		

REFERENCES

- Biberman, L. M. *Perception of Displayed Information*. Plenum Press, New York, 1973.
- Bonnett, D. G. Microdensitometric prediction of the recognition of real objects. Unpublished Master's thesis, Virginia Polytechnic Institute and State University, 1975.
- DePalma, J. J. and Lowry, E. M. "Sine-Wave Response fo the Visual System. II. Sine-Wave and Square-Wave Contrast Sensitivity." *Journal of the Optical Society of America*, 1962, 52, 328-335.
- Evans, J. E., III and Gutmann, J. C. "Minicomputer Processing of Dual Purkinje Image Eye-Tracker Data." *Behavior Research Methods and Instrumentation*, 1978, 10, 701-704.
- Gould, J. "Eye-Movements during Visual Search." In H. Leibowitz (Ed.), *NATO Symposium of Image Evaluation*, Munich, 1969, 145-161.
- Hershey, H. C., Zakin, J. L., and Simha, R. "Numerical Differentiation of Equally Spaced and Not Equally Spaced Experimental Data." *Industrial and Engineering Chemistry Fundamentals*, 1967, 6, 413-420.
- Humes, J. M. and Bauerschmidt, D. K. *Low Light Level TV Viewfinder Simulation Program, Phase B Report*. Avionics Laboratory, Wright-Patterson AFB, OH, Report No. AFAL-TR-68-271, November, 1968.
- Keesee, R. L. *Prediction of Modulation Detectability Thresholds for Line-Scan Displays*. Aerospace Medical Research Laboratory, Wright-Patterson AFB, OH, Report No. AMRL-TR-76-38, December, 1976.
- Maddox, M. E. Prediction of information transfer from computer-generated dot matrix displays. Unpublished Master's thesis, Virginia Polytechnic Institute and State University, 1977.
- Rosell, F. A. and Willson, R. H. "Recent Psychophysical Experiments and the Display Signal-to-Noise Ratio Concept." In L. M. Biberman (Ed.), *Perception of Displayed Information*, Plenum Press, New York, 1973.
- Savitsky, A. and Golay, M. J. E. "Smoothing and Differentiation of Data by Simplified Least Squares Procedures." *Analytical Chemistry*, 1964, 36, 1627-1639.
- Schade, O. H. "Image Reproduction by a Line Raster Process." In L. M. Biberman (Ed.), *Perception of Displayed Information*, Plenum Press, New York, 1973.

Schindler, R. A. and Martin, W. L. *Optical Power Spectrum Analysis of Display Imagery*. Aerospace Medical Research Laboratory, Wright-Patterson AFB, OH, Report No. AMRL-TR-78-50, June, 1978.

Snyder, H. L. "Image Quality and Observer Performance." In L. M. Biberman (Ed.), *Perception of Displayed Information*. Plenum Press, New York, 1973.

Snyder, H. L. *Visual Search and Image Quality: Final Report*. Aerospace Medical Research Laboratory, Wright-Patterson AFB, OH, Report No. AMRL-TR-76-89, December 1976.

Snyder, H. L., Keesee, R. L., Beamon, W. S., and Aschenbach, J. R. *Visual Search and Image Quality*. Aerospace Medical Research Laboratory, Wright-Patterson AFB, OH, Report No. AMRL-TR-73-114 (AD A-007375).

Snyder, H. L., and Taylor, D. F. *Computerized Analysis of Eye Movements During Static Display Visual Search*. Aerospace Medical Research Laboratory, Wright-Patterson AFB, OH, Report No. AMRL-TR-75-91, February 1976.

Steiner, J., Termonia, Y., and Deltour, J. "Comments on Smoothing and Differentiation of Data by Least Squares Procedure." *Analytical Chemistry*, 1972, 44, 1906-1909.

Task, L. H. *An Evaluation and Comparison of Several Measures of Image Quality for Television Displays*. Aerospace Medical Research Laboratory, Wright-Patterson AFB, OH, Report No. AMRL-TR-79-7, January 1979.